

**SWAY CHARACTERISTICS OF BRICK INFILLED REINFORCED  
CONCRETE BUILDING FRAME UNDER LATERAL LOADING**

**M.Engg. Project**



by

**Abdul Waset**

**Roll no-9404329**

**Submitted to the Department of Civil Engineering  
Bangladesh University of Engineering and Technology,  
in partial fulfillment of the requirements for the degree  
of**

**Master of Engineering in Civil Engineering (Structural)**

**2002**



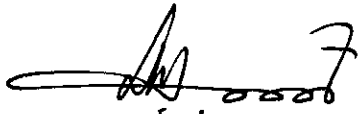
**SWAY CHARACTERISTICS OF BRICK INFILLED REINFORCED  
CONCRETE BUILDING FRAME UNDER LATERAL LOADING**

**M.Engg.Project by**

**ABDUL WASET**

**Roll: 9404329**

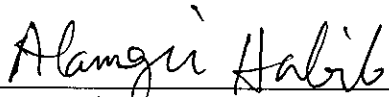
Approved as to the style and content as M.Engg.project report on 15 th April, 2002  
by



---

Dr. Khan Mahmud Amanat  
Associate Professor  
Department of Civil Engineering  
BUET, Dhaka.

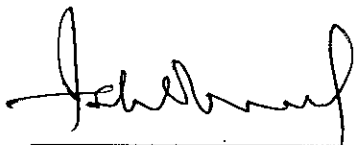
Chairman  
(Supervisor)



---

Dr. Alamgir Habib  
Professor  
Department of Civil Engineering  
BUET, Dhaka.

Member



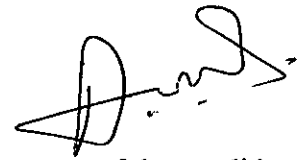
---

Dr. Ishtiaque Ahmed  
Associate Professor  
Department of Civil Engineering  
BUET, Dhaka.

Member

## DECLARATION

Declared that the work embodied in the thesis of the work has been carried out by the author under the supervision of Dr. Khan Mahmud<sup>h</sup>Amanat, Associate Professor, Department of Civil Engineering, Bangladesh University of Engineering and Technology. It is hereby declared that this thesis or any part of it has not been submitted elsewhere for the award of any degree or diploma.

A handwritten signature in black ink, appearing to be 'D. Amanat', written in a cursive style.

Signature of the candidate

## TABLE OF CONTENTS

List of symbols

List of figures

List of graphs

Acknowledgement

Abstract

### Chapter 1 : INTRODUCTION

|                                |   |
|--------------------------------|---|
| 1.1 General                    | 1 |
| 1.2 Frames with infill         | 2 |
| 1.3 Objective and scope        | 3 |
| 1.4 Organization of the thesis | 3 |

### Chapter 2 : INFILLED FRAME STRUCTURES

|   |    |
|---|----|
| 2.1 Introduction                                | 5  |
| 2.2 Behavior of infilled frames                 | 5  |
| 2.3 Overview of the analysis of infilled frames | 8  |
| 2.3.1 Approximate method                        | 9  |
| 2.3.2 Equivalent strut method                   | 12 |
| 2.3.3 Plasticity model                          | 14 |
| 2.3.4 Coupled boundary element method           | 16 |
| 2.3.5 Choice of the model                       | 16 |
| 2.4 Equivalent strut modeling                   | 16 |
| 2.5 Beam and column moment capacity             | 18 |
| 2.6 Determination of $K_0$                      | 20 |

### Chapter 3 : COMPUTATIONAL MODELING OF INFILLED FRAMES

|                  |    |
|------------------|----|
| 3.1 Introduction | 28 |
|------------------|----|

|       |  |    |
|-------|--|----|
| 3.2   | The finite element package                 | 28 |
| 3.3   | Finite element modeling of infilled frames | 29 |
| 3.3.1 | Modeling of beams and columns              | 30 |
| 3.3.2 | Modeling of infill                         | 32 |
| 3.4   | Loads                                      | 34 |
| 3.5   | Developing finite element mesh             | 40 |
| 3.6   | Typical analysis results                   | 40 |
| 3.6.1 | Typical outputs                            | 47 |

#### **Chapter 4 : SENSITIVITY ANALYSIS AND DISCUSSION**

|       |   |    |
|-------|---|----|
| 4.1   | Introduction                            | 56 |
| 4.2   | Study parameters                        | 56 |
| 4.2.1 | Friction co-efficient $\mu$             | 57 |
| 4.2.2 | Masonry compressive strength $f'_m$     | 57 |
| 4.2.3 | Panel aspect ratio                      | 57 |
| 4.2.4 | Column stiffness                        | 57 |
| 4.2.5 | Wall thickness $t$                      | 58 |
| 4.2.6 | Masonry ultimate strain $\epsilon'_m$   | 58 |
| 4.3   | Observation parameters                  | 58 |
| 4.4   | Results and discussion                  | 58 |
| 4.4.1 | Sensitivity of $K_0$                    | 58 |
| 4.4.2 | Sensitivity study of deflection         | 60 |
| 4.5   | Behavior of frame in presence of infill | 61 |

#### **Chapter 5 : CONCLUSIONS**

|     |   |    |
|-----|---|----|
| 5.1 | General                                     | 73 |
| 5.2 | Conclusions                                 | 73 |
| 5.3 | Recommendation for the future investigation | 74 |

## LIST OF SYMBOLS

- $\tau_{xy}$  : Shear stress, N/mm<sup>2</sup>
- $\sigma_y$  : Vertical compressive stress, N/mm<sup>2</sup>
- $Q$  : Horizontal shear load, N
- $l'$  : Length of infill in mm
- $h'$  : Height of infill in mm
- $t$  : Wall thickness in mm
- $\sigma_d$  : Diagonal tensile stress, N/mm<sup>2</sup>
- $E_m$  : Elastic modulus of masonry, N/mm<sup>2</sup>
- $E_l$  : Flexural rigidity of column, N/mm<sup>2</sup>
- $\lambda$  : The parameter expressing the bearing stiffness of the infill relative to the flexural rigidity of the column.
- $f'_m$  : Masonry compressive strength, MPa
- $Q'_c$  : Ultimate horizontal shear, N
- $Q_c$  : Allowable horizontal shear, N
- $V_m$  : Maximum lateral force, N
- $u_m$  : Maximum lateral displacement, mm
- $\epsilon'_m$  : Masonry ultimate strain, mm
- $\theta$  : Inclination of the diagonal strut Degree
- $v$  : Basic shear strength, MPa
- $A_d$  : Area of equivalent diagonal strut, mm<sup>2</sup>
- $L_d$  : Length of equivalent diagonal strut, mm
- $K_\theta$  : The initial stiffness of infill, N-mm
- $M_{pc}$  : Plastic resisting moment of column, N-mm
- $M_{pb}$  : Plastic resisting moment of beam, N-mm
- $M_{pj}$  : Plastic resisting moment of beam and column joint, N-mm
- $r$  : Aspect ratio of the frame

- $h$  : Centre to center height of beam, mm  
 $l$  : Centre to center length of column, mm  
 $\phi$  : A constant value 0.65  
 $\sigma_{c0}$  : Normal stress in column, N/mm<sup>2</sup>  
 $\sigma_{b0}$  : Normal stress in beam, N/mm<sup>2</sup>  
 $f'_c$  : Effective compressive strength of masonry, N/mm<sup>2</sup>  
 $\mu$  : Co-efficient of friction between frame and infill interface  
 $\alpha_c$  : Normalized length of contact for column  
 $\alpha_b$  : Normalized length of contact for beam  
 $\beta_0$  : A reduction factor 0.2  
 $A_c$  : Contact normal stress area in column, mm<sup>2</sup>  
 $A_b$  : Contact normal stress area in beam, mm<sup>2</sup>  
 $\sigma_c$  : The real normal contact stress in column, N/mm<sup>2</sup>  
 $\sigma_b$  : The real normal contact stress in beam, N/mm<sup>2</sup>  
 $\tau_b$  : Nominal contact shear stress in beam, N/mm<sup>2</sup>  
 $\tau_c$  : Nominal contact shear stress in column, N/mm<sup>2</sup>  
 $f_a$  : Actual compressive strength of masonry, MPa  
 $v_b$  : Basic wind speed, Km/h  
 $C_p$  : Overall pressure co-efficient  
 $C_G$  : Gust response factor  
 $C_C$  : Velocity to pressure conversion co-efficient  $47.2 \times 10^{-6}$   
 $C_I$  : Structural importance co-efficient  
 $C_Z$  : Combined height and exposure co-efficient  
 $q_z$  : Sustained wind pressure, N/mm<sup>2</sup>  
 $p_z$  : Design wind pressure, N/mm<sup>2</sup>

## LIST OF FIGURES

|          |  |    |
|----------|--|----|
| Fig 1.1  | Structural frame infilled with masonry                         | 2  |
| Fig 2.1  | Interactive behavior of frame and infill                       | 6  |
| Fig 2.2  | Analogous braced frame   | 6  |
| Fig 2.3  | Modes of infill failure  | 7  |
| Fig 2.4  | Modes of frame failure   | 8  |
| Fig 2.5  | Masonry infill frame subassemblage in masonry infill panel     |    |
|          | Frame structures   | 13 |
| Fig 2.6  | Masonry infill panel in frame structures                       | 13 |
| Fig 2.7  | Constitutive model for masonry infill panel                    | 14 |
| Fig 2.8  | Strength envelope for masonry infill panel                     | 14 |
| Fig 2.9  | Proposed composite yield criterion with iso-shear stress lines | 15 |
| Fig 2.10 | Typical layout of reinforcement in column for 11 story frame   | 20 |
| Fig 2.11 | Typical layout of reinforcement in column for 7 story frame    | 20 |
| Fig 2.12 | Typical layout of reinforcement in beam                        | 21 |
| Fig 2.13 | Frame forces equilibrium                                       | 21 |
| Fig 3.1  | Beam4 3-D elastic beam   | 30 |
| Fig 3.2  | COMBIN39 Nonlinear spring                                      | 32 |
| Fig 3.3  | Plan of structure  | 36 |
| Fig 3.4  | Elevation of 7 story building                                  | 37 |
| Fig 3.5  | Elevation of 11 story building                                 | 38 |
| Fig 3.6  | Finite element modeling of 7 story infilled frame              | 46 |
| Fig 3.7  | Finite element modeling of 7 story frame without infill        | 47 |
| Fig 3.8  | Finite element modeling of 11 story infilled frame             | 48 |
| Fig 3.9  | Finite element modeling of 11 story frame without infill       | 49 |
| Fig 3.10 | Deflected shape of 7 story infilled frame                      | 50 |
| Fig 3.11 | Deflected shape of 7 story frame without infill                | 51 |
| Fig 3.12 | Deflected shape of 11 story infilled frame                     | 52 |
| Fig 3.13 | Deflected shape of 11 story frame without infill               | 53 |

## LIST OF GRAPHS

|           |  |    |
|-----------|--|----|
| Fig 4.1   | Variation of diagonal strut stiffness with masonry ultimate strain for 11 storied frame  | 61 |
| Fig 4.2.a | Variation of diagonal strut stiffness with compressive strength of masonry when infill thickness is 250 mm for 7 storied frame           | 62 |
| Fig 4.2.b | Variation of diagonal strut stiffness with compressive strength of masonry when infill thickness is 150 mm for 7 storied frame           | 62 |
| Fig 4.3.a | Variation of diagonal strut stiffness with co-efficient of friction between frame and infill interface for 7 story 150 mm infilled frame | 63 |
| Fig 4.3.b | Variation of diagonal strut stiffness with co-efficient of friction between frame and infill interface for 7 story 250 mm infilled frame | 63 |
| Fig 4.4.a | Variation of diagonal strut stiffness with column stiffness for 150 mm infilled frame  | 64 |
| Fig 4.4.b | Variation of diagonal strut stiffness with column stiffness for 250 mm infilled frame  | 64 |
| Fig 4.5.a | Variation of diagonal strut stiffness with panel aspect ratio for 7 storied frame  | 65 |
| Fig 4.5.b | Variation of diagonal strut stiffness with panel aspect ratio for 11 storied frame   | 65 |
| Fig 4.6.a | Variation of lateral deflection with co-efficient of friction between frame and infill interface for 11 story frame                      | 66 |
| Fig 4.6.b | Variation of lateral deflection with co-efficient of friction between frame and infill interface for 7 story frame                       | 66 |
| Fig 4.7.a | Variation of lateral deflection with compressive strength of masonry for 11 story frame  | 67 |
| Fig 4.7.b | Variation of lateral deflection with compressive strength of masonry for 7 story frame   | 67 |
| Fig 4.8.a | Variation of deflection with panel aspect ratio for 7 storied  |    |

|            |   |    |
|------------|---|----|
|            | frame   | 68 |
| Fig 4.8.b  | Variation of deflection with panel aspect ratio for 11 storied Frame        | 68 |
| Fig 4.9.a  | Variation of deflection with column stiffness for infill Thickness 150 mm   | 69 |
| Fig 4.9.b  | Variation of deflection with column stiffness for infill Thickness 250 mm   | 69 |
| Fig 4.10.a | Variation of deflection with masonry ultimate strain for 11 storied frame   | 70 |
| Fig 4.10.b | Variation of deflection with masonry ultimate strain for 7 storied frame    | 70 |
| Fig 4.11.a | Variation of floor height with deflection/total height for 7 storied frame  | 71 |
| Fig 4.11.b | Variation of floor height with deflection/total height for 11 storied frame | 71 |

## ACKNOWLEDGEMENT

This study was undertaken under the supervision of Dr. Khan Mahmud Amanat, Associate Professor, Department of Civil Engineering, Bangladesh University of Engineering and Technology. His systematic guidance and constant persuasion has helped the author at all stages of this project. The author sincerely acknowledge his heartiest gratitude and indebtedness to Dr. Khan Mahmud Amanat for his superior technical expertise, impromptu answers and solutions to any project related problems.

The author also pays his deepest homage to his family members for their inspiration. The author is grateful to his office colleagues who helped him by sharing his office duties and thereby giving opportunities for study.

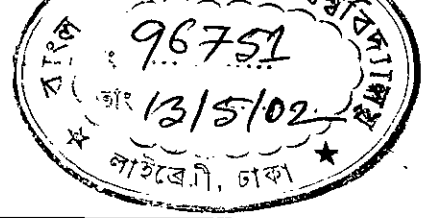
## ABSTRACT

Frame structure is most common in tall buildings due to simplicity in design and construction. In Bangladesh brick walls are used in frame structures as exterior walls and partitions. Present code of practice does not include provision of taking into consideration the structural effect of infill in multistoried building construction. The presence of infill increases the lateral stiffness of the structure and reduces the amount of deflection. If this effect is taken into consideration, the resulting structure will be economic.

This study has been undertaken to investigate the sway characteristics of common reinforced concrete frames in presence of brick masonry infill subjected to lateral loads. Here, a seven story and an eleven story building frames are taken as reference structures. Finite element modeling is used to model the frame. Common three dimensional frame elements are used to model the beams and columns. The in-plane stiffness of brick wall contributing to the stiffness of the frame against lateral load is modelled by the *equivalent strut model* proposed by Saneinejad and Hobbs (1995). Their model consisted of a bi-linear force-displacement relationship with an initial stiffness called  $K_0$ . In this study, instead of the bi-linear relationship, a non-linear constitutive relation is proposed and used to simulate the force vs. displacement behavior of the diagonal strut as infill. In the FE model the struts are incorporated using special link element having only axial stiffness. Lateral loads (wind load) are calculated as described in BNBC, 1993.

A parametric study was performed using various parameters of frame and infill to see their effects on stiffness properties of infill and deflection characteristics of the frame. A few parameters are found to have significant effect on the infill characteristics while the other parameters do not have any appreciable effect. While

studying the deflection characteristics, it is observed that deflection in frames with infill is much smaller than that with frames without infill. On the average, lateral sway is reduced by about thirty percent if only one third of the panels of the frames contain infill. It proves that the sway predicted by ordinary frame analysis overestimates the sway by a significant amount. A suggestion is thus made that after computing sway by a ordinary frame analysis, it may be reduced by at least thirty percent before it is compared with the maximum allowable sway specified by code.



---

**CHAPTER 1**  
**INTRODUCTION**

---

### **1.1 GENERAL**

Frame structures are frequently used in multistoried building construction. It is mainly due to ease in construction and rapid progress of work. In these frames infills are used as exterior and partition walls. In Bangladesh, generally the infill exterior and partition walls are made of brick masonry and present code of practice does not include the effect of infill. Lateral deflection of frame is considered as one of the principal design criteria for designing tall building structures. Which depends on the following characteristics of frame:

- 1) Column stiffness,
- 2) Beam stiffness and
- 3) The stiffness of the infill wall.

Generally the column stiffness and beam stiffness are taken into consideration when the lateral deflection is calculated in the frame under lateral load ignoring infill stiffness. In presence of infill the stiffness of the frame is more and deflection would be less. In frame without infill, the stiffness is less and hence deflection is more.

Present code of practices does not include provision of taking into consideration the effect of infill. It is understood that if the effect of infill is taken into account in the design of frame, the resulting structures would be significantly different. A number of researches like Mander et al. (1993). Holmes (1961), Stafford Smith and Carter (1969) and recently Saneinejad and Hobbs (1995) addressed this problem and suggested a number of methods to take into account the effect of infill in the analysis of design. However all these methods consider only the stone masonry infill.

Brick made from burning clay is a unique construction material available in this sub continent. It is used widely in our country as one of the principal construction

material due to insufficient availability of stones. Generally in all framed structures in our country, brick is used for partition walls, which also acts as infill to the frame. Inadequate knowledge of the mechanical properties of brick masonry prohibit us from considering infills as a structural element, although it is apparent that brick infills have significant in-plane stiffness contributing to the stiffness of the frames against lateral load. It is therefore necessary to understand the characteristics of brick masonry infilled RC frame in order to exploit the full potential of the structural properties of the infill. With this objective in mind, an investigation is performed to understand the behavior of brick masonry infill in building frames.

## 1.2 FRAMES WITH INFILL

The infilled frame consists of a steel or reinforced concrete column and girder frame with infills of brick work or concrete block work as shown in fig 1.1.

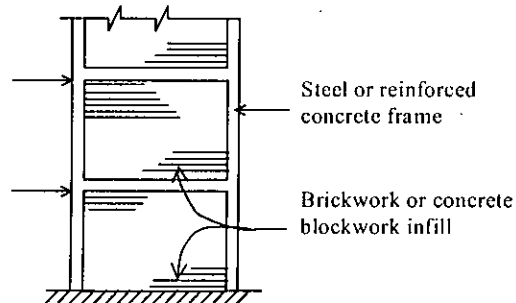


Fig 1.1 Structural frame infilled with masonry

In countries ( Smith and Coull,1985) with stringently applied codes of practice the absence of a well recognized method of design for infilled frames has severely restricted their use as bracing frame. It has been more usual in such countries, when designing an infilled frame structure to arrange for the frame to carry the total vertical and horizontal loading and to include the infills on the assumptions that, with precautions taken to avoid load being transferred to them, the infills do not participate as part of the primary structure. It is evident from the frequently observed diagonal cracking of such infill walls that the approach is not

always wise. The walls do sometimes attract significant bracing loads and, in so doing, modify the structures mode of behavior and the forces in the frame. In such cases it would have been better to design the walls for the lateral loads, and the frame to allow for its modified mode of behavior.

Certain reservations arise in the use of infilled frames for bracing a structure. For example, it is possible that as part of a renovation project, partition walls are removed with the result that the structure becomes inadequately braced. Precautions against this, either by including a generously excessive number of bracing walls, or by somehow permanently identifying the vital bracing walls, should be considered as part of the design.

### **1.3 OBJECTIVE AND SCOPES**

The objective of this thesis is to investigate the sway characteristics of common reinforced concrete frames in presence of brick masonry infill subjected to lateral loads. To carry out a systematic investigation, various parameters shall be studied to understand their relative influence on the behavior of infill as well as on the frame. Comparative study shall be made with similar frames without infill to establish the contribution of infill in changing the sway behavior of RC frames.

The study shall be limited to the investigation of frames subjected to wind loading. 2D investigation of 3D frames shall be used. The infill shall be modeled as a diagonal strut following the model proposed by Saneinejad and Hobbs (1995). A non-linear force-displacement relationship for the diagonal strut shall be used based on a proposed non-linear equation for the constitutive relation.

### **1.4 ORGANIZATION OF THIS THESIS**

The whole thesis is organized into five chapters. Chapter 1 is the current chapter which introduces the work presented in this thesis. Chapter 2 deals with the infilled frame structure which include the characteristics of infilled frame and different method for analysis of infilled frame. Chapter 3 discuss about the computational modeling of infilled frames using finite element technique. Chapter 4.

is aimed at the sensitivity analysis and discussion based on various parameters of infilled frames. And finally, chapter 5 draws a conclusion by summarizing the outcome of the thesis and proposed new direction for further research and development.

---

**CHAPTER 2**  
**INFILLED FRAME STRUCTURE**

---

### **2.1 INTRODUCTION**

Frame structures with masonry infill are most common form of high rise construction in non-earthquake regions where the wind forces are not severe. Masonry infill panels are frequently found as interior and exterior partitions in RC frame structures. In most of the cases infills are assumed not to participate as a part of the primary structure. This is because of the absence of a well-recognized method of design for infilled frames. The significance of infilling walls in determining the actual strength and stiffness of framed buildings subjected to lateral force has long been recognized. Despite rather intensive investigations during the last decades, the inclusion of infilling walls as structural elements is not yet common, because of the design complexity and lack of suitable theory. During the same period, analysis and design of multistory frames have developed rapidly. According to the latest developments, the  $P-\Delta$  effect in a fully restrained multistory frame is a major design factor. The more flexible the frame, the greater the secondary bending moments become. Therefore, the influence of infilling walls is much more significant today than in the past, because they provide lateral stiffness and minimize the  $P-\Delta$  effect. They can also provide significant lateral strength.

### **2.2 BEHAVIOUR OF INFILLED FRAMES**

The behavior of masonry infilled frames has been extensively studied in the last four decades in attempts to develop a rational approach for design of such frames. The use of a masonry infill to brace a frame combines some of the desirable structural characteristics of each, while overcoming some of their deficiencies. The high in-plane rigidity of the masonry wall significantly stiffens the otherwise relatively flexible frame, while the ductile frame contains the brittle masonry, after cracking, upto loads and displacements much larger than it could achieve without frame. The result is, therefore, a relatively stiff and tough bracing system.

The wall braces the frame partly by its in-plane shear resistance and partly by its behavior as a diagonal bracing strut in the frame. Fig 2.1 shows such modes of behavior.

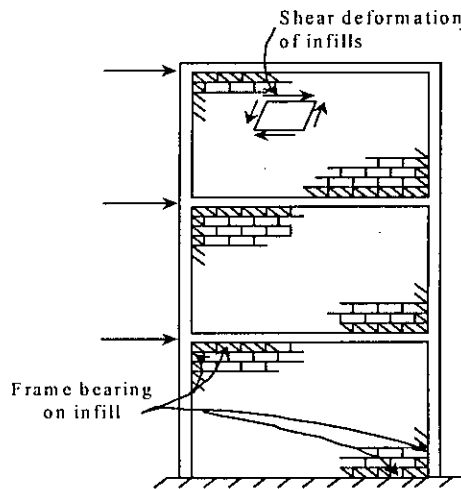


Fig 2.1 Interactive behavior of frame and infill

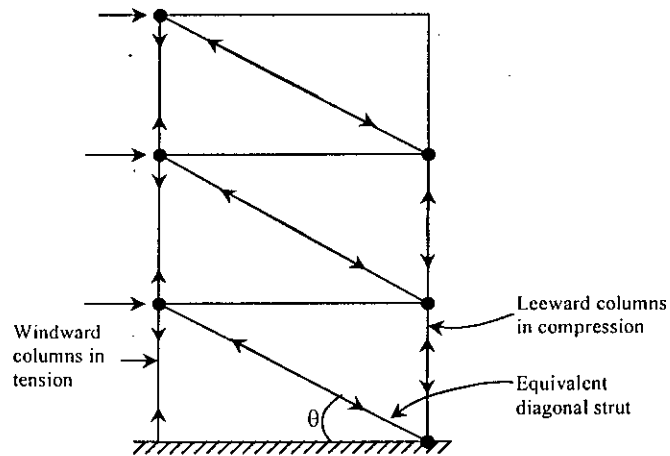


Fig 2.2 Analogous braced frame

When the frame is subjected to horizontal loading, it deforms with double-curvature bending of the columns and beams. The translation of the upper part of the column in each story and the shortening of the leading diagonal of the frame cause the column to lean against the wall as well as to compress the wall along its diagonal. It is roughly analogous to a diagonally braced frame ( Fig 2.2 ).

Three potential modes of failure of the wall arise as a result of its interaction with the frame. These are given below:

1. Shear failure
2. Diagonal cracking of the wall
3. Compression failure

These are shown in fig 2.3. The modes of frame failure are as follows:

1. Tension failure and
2. Flexure or shear failure

These are shown in fig 2.4.

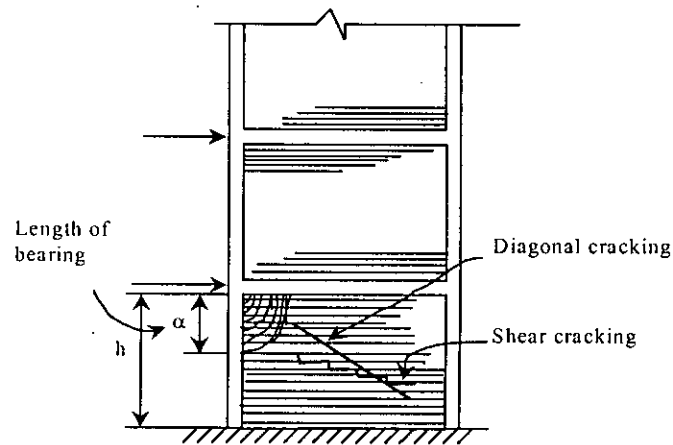


Fig 2.3 Modes of infill failure

The shear failure of wall steps down through the joints of the masonry, and precipitated by the horizontal shear stresses in the bed joints. The diagonal cracking of the wall is through the masonry along a line, or lines, parallel to the leading diagonal, and caused by tensile stresses perpendicular to the leading diagonal. The 'perpendicular' tensile stresses are caused by the divergence of the compressive stress trajectories on opposite sides of the leading diagonal as they approach the middle region of the infill. The diagonal cracking is limited at and spreads from the middle of the infill, where the tensile stresses are a maximum, tending to stop near the compression corners, where the tension is suppressed. In compression failure, a

corner of the infill at one of the ends of the diagonal strut may be crushed against the frame due to the high compressive stresses in the corner.

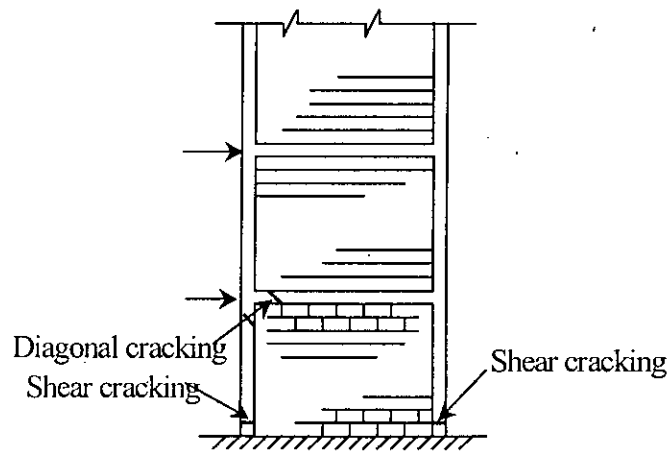


Fig 2.4 Modes of frame failure

The nature of the forces in the frame can be understood by referring to the analogous braced frame ( Fig 2.2). the windward column is in tension and the leeward column is in compression. Since the infill bears on the frame not as a concentrated force exactly at the corner, the frame members are subjected also to transverse shear and a small amount of bending. Consequently, the frame members or their connections are liable to fail by axial force or shear and especially by tension at the base of the windward column (Fig 2.4).

### 2.3 OVERVIEW OF THE ANALYSIS OF INFILLED FRAMES

Attempts to the analysis and design of infilled frames since the mid-1950 have led to several methods. Holmes (1961) replaced the infill by an equivalent pin-jointed diagonal strut made of the same material and having a width of one third of the infill diagonal .Stafford Smith (1966) and Stafford Smith and Carter (1969) related the width of the equivalent diagonal strut to the infill frame stiffness parameters.

Because the elastic methods could not fully represent the actual behavior of infilled frames, attention was paid to the theories of plasticity. Wood (1978) extended the limit analysis of plasticity with the assumption of perfect plasticity.

Recently a method was developed by Saneinejad (1990) that allows for interface shear forces and both the elastic and plastic behavior of material.

The theory of plasticity, which is adopted to describe the inelastic behavior, utilizes modern algorithmic concepts, including an implicit Euler backward return mapping scheme, a local Newton-Raphson and a consistent tangential stiffness matrix. The stiffness of the structural system is determined with variations in geometrical and mechanical characteristics. The analysis is carried out utilizing the boundary element method (BEM) for the infill and dividing the frame into finite elements, so as to transform the mutual interactions of the two subsystems into stresses distributed along the boundary for the infill and into nodal actions for the frame.

### 2.3.1 Approximate Method (Smith and Coull, 1985)

A concept of the behavior of infilled frames has been developed from approximate analysis. An understanding of infilled-frame behavior is far from complete and further research needs to be done, especially with full-scale tests. Consequently, opinions about the approach to the design of infilled frames differ, especially as to whether it should be elastically or plastically based. The method presented here draws from a combination of test observations and the results of analysis. It may be classified as an elastic approach except for the criterion used to predict the infill crushing, for which a plastic type of failure of the masonry infill is assumed.

#### Stresses in the infill

*Relating to shear failure:* Shear failure of the infill is related to the combination of shear and normal stresses induced at points in the infill when the frame bears on it as the structure is subjected to the external lateral shear. An extensive series of plane-stress membrane finite-element analysis has shown that the critical values of this combination of stresses occur at the center of the infill and that they can be expressed empirically by,

$$\text{Shear stress } \tau_{xy} = \frac{1.43Q}{Lt} \quad 2.1$$

$$\text{Vertical compressive stress } \sigma_y = \frac{(0.8h/L - 0.2)Q}{Lt} \quad 2.2$$

Where  $Q$  is the horizontal shear load applied by the frame to the infill of length  $L$ , height  $h$ , and thickness  $t$ .

**Relating to diagonal tensile failure** : Diagonal cracking of the infill is related to the maximum value of diagonal tensile stress in the infill. This also occurs at the center of the infill and, based on the results of the analyses, may be expressed empirically as

$$\text{Diagonal tensile stress } \sigma_d = \frac{0.58Q}{Lt} \quad 2.3$$

These stresses are governed mainly by the proportions of the infill. They are little influenced by the stiffness properties of the frame because they occur at the center of the infill, away from the region of contact with the frame.

**Relating to the compressive failure of the corner**: Tests on model infilled frames have shown that the length of bearing of each story-height column against its adjacent infill is governed by the flexural stiffness of the column relative to the inplane bearing stiffness of the infill. The stiffer the column, the longer the length of bearing and the lower the compressive stresses at the interface. Tests to failure have borne out the deduction that the stiffer the column, the higher the strength of the infill against compressive failure. They have also shown that crushing failure of the infill occurs over a length approximately equal to the length of bearing of the column against the infill (Fig 2.3).

As a crude approximation, an analogy may be drawn with the theory for a beam on an elastic foundation, from which it has been proposed that the length of column bearing  $\alpha$  may be estimated by

$$\alpha = \frac{\pi}{2\lambda} \quad 2.4$$

$$\text{where, } \lambda = \sqrt{\frac{E_m t}{4EIh}} \quad 2.5$$

in which  $E_m$  is the elastic modulus of masonry and  $EI$  the flexural rigidity of the column.

The parameter  $\lambda$  expresses the bearing stiffness of the infill relative to the flexural rigidity of the column: the stiffer the column, the smaller the value of  $\lambda$  and longer the length of bearing.

It is assumed that when the corner of the infill crushes, the masonry bearing against the column within the length  $\alpha$  is at the masonry ultimate compressive stress  $f'_m$ , then the corresponding ultimate horizontal shear  $Q'_c$  on the infill is given by

$$Q'_c = f'_m \alpha t \quad 2.6$$

$$\text{or, } Q'_c = f'_m t \cdot \frac{\pi}{2} \sqrt{\frac{4EIh}{E_m t}} \quad 2.7$$

Considering now the allowable horizontal shear  $Q_c$  on the infill, and assuming a value for  $E/E_m$  of 30 in the case of steel frame and 3 in the case of reinforced concrete frame, the allowable horizontal shear on a steel framed infill corresponding to a compressive failure is given by

$$Q'_c = 5.2 f'_m \sqrt[4]{Iht^3} \quad 2.8$$

and for a reinforced concrete infill

$$Q'_c = 2.9 f'_m \sqrt[4]{Iht^3} \quad 2.9$$

These semi empirical formulas indicate the significance of parameters that influence the horizontal shear strength of an infill when it is governed by a compressive failure of one of its corner. The masonry compressive strength and the wall thickness have the most direct influence on the infill strength, while the column inertia and infill height exert control in proportion to their fourth roots. The infill strengths indicated by equations 2.8 and 2.9 are very approximate. Experimental evidence has shown them to overestimate the real values; therefore, they will be modified before being used in the design procedure.

### 2.3.2 Equivalent Strut Method

Saneinejad and Hobbs (1995) developed a method based on the equivalent diagonal strut approach for the analysis and design of steel or concrete frames with concrete or masonry infill walls subjected to in-plane forces. The method takes into account the elastoplastic behavior of infilled frames considering the limited ductility of infill materials. Various governing factors such as the infill aspect ratio, the shear stresses at the infill-frame interface, and relative beam and column strengths are accounted for in this development.

The proposed analytical development assumes that the contribution of the masonry infill panel (shown in fig 2.5) to the response of the infilled frame can be modeled by replacing the panel by a system of two diagonal masonry compression struts (fig 2.6). The stress-strain relationship for masonry in compression (fig 2.7), used to determine the strength envelope of the equivalent strut, can be idealized by a polynomial function. Since the tensile strength of masonry is negligible, the individual masonry struts are considered to be ineffective in tension. However, the combination of both diagonal struts provides a lateral load resisting mechanism for the opposite lateral directions of loading.

The lateral force-deformation relationship for the structural masonry infill panel is assumed to be a smooth curve bounded by a bilinear strength envelope with an initial elastic stiffness until the yield force  $V_y$  and there on a postyield degraded stiffness until the maximum force  $V_m$  is reached (fig 2.8). The corresponding lateral displacement values are denoted as  $u_y$  and  $u_m$  respectively. The analytical formulations for the strength envelope parameters were developed on the basis of the available "equivalent strut model" for infilled masonry frames.

### 2.3.3 Plasticity Model (Lourenco et al.1997)

The theory of plasticity, which is adopted to describe the inelastic behavior, utilizes modern algorithmic concepts, including an implicit Euler background return mapping scheme, a local Newton-Raphson method and a consistent tangential stiffness matrix. The model is capable of predicting independent response along the material axes. It features a tensile fracture energy and a compressive fracture energy, which are different for each material axis.

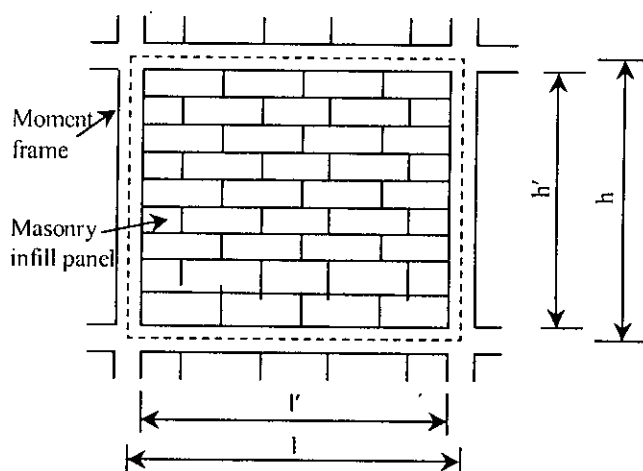


Fig 2.5 Masonry infill frame subassemblage in masonry infill panel frame structures.

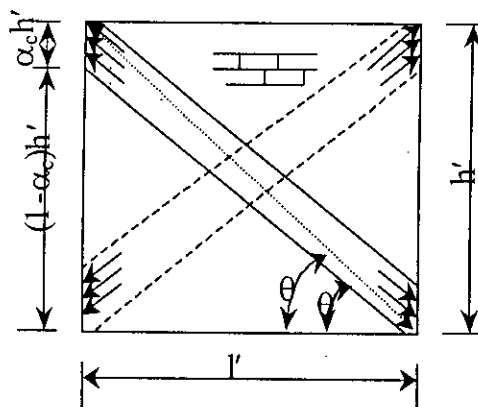


Fig 2.6 Masonry infill panel in frame structures.

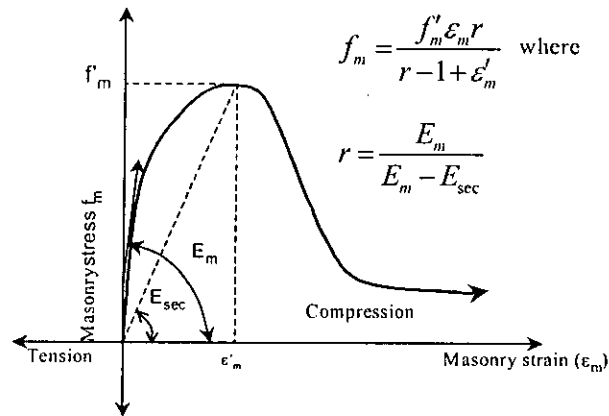


Fig 2.7 Constitutive model for masonry infill panel (Saneinejad,1995)

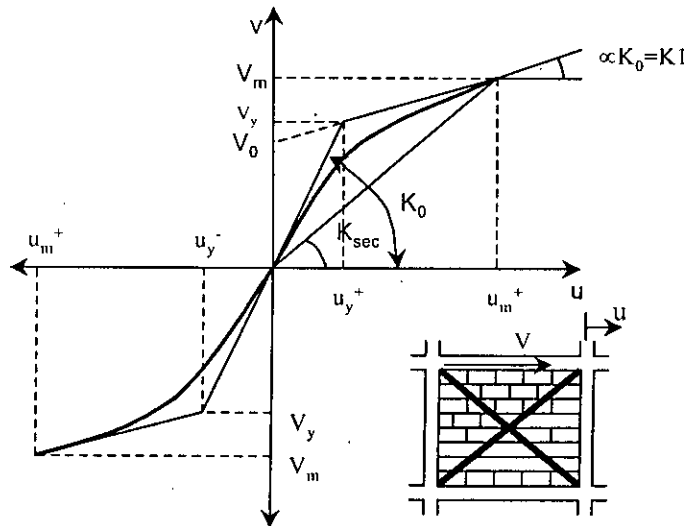


Fig 2.8 Strength envelope for masonry infill panel (Saneinejad,1995)

A large number of anisotropic materials exist in engineering such as masonry, plastics, wood and most composites. The framework of plasticity theory is general enough to apply to both isotropic and anisotropic behavior. Indeed, the past decade has witnessed numerous publications on second numerical implementations of isotropic plasticity models. Nevertheless, it appears that, while some anisotropic plasticity models have been proposed from purely theoretical and experimental standpoints, only a few numerical implementations and calculations have actually been carried out. Examples include the work of de Borst and Feenstra (1990) and Schellekens and de Borst (1990) who fully treated the implementation of elastic-

perfectly-plastic Hill (1948) and Hoffman (1967) criteria, respectively. In these publications hardening behavior has been simulated with the fraction model of Besseling (1958). More recently, linear tensorial hardening has been incorporated in the hill criterion. It is not surprising that only a few anisotropic models have been implemented and tested successfully. An accurate analysis of anisotropic materials requires a description for all stress states. The yield criterion proposed in this study combines the advantages of modern plasticity concepts with a powerful representation of anisotropic material behavior, which includes different hardening / softening behavior along each material axis.

In order to model orthotropic material behavior, a Hill-type criterion (1948) for compression and a Rankine-type criterion for tension are proposed (fig 2.9). The internal damage due to these failure mechanisms is represented with two internal parameters, one for damage in tension and one for damage in compression. The model is formulated in such a way that each internal parameter is related to two independent fracture energies along each material axis.

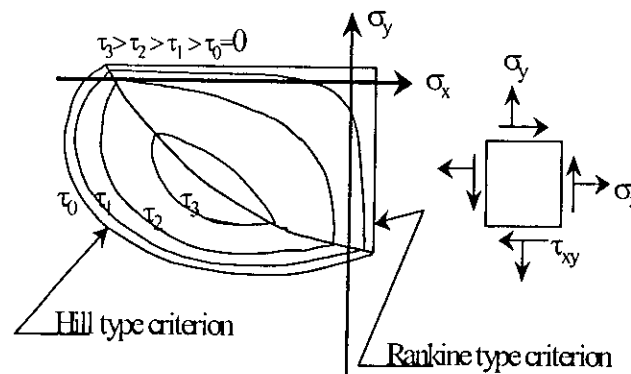


Fig 2.9 Proposed composite yield criterion with iso-shear stress lines .

#### 2.3.4 Coupled Boundary Element Method (Papia,M.1988)

The behavior of infilled frames subjected to horizontal loads is analysed by an iterative numerical procedure. The stiffness of the structural system is determined with variations in geometrical and mechanical characteristics.

The stiffness contribution by brickwork or concrete panels in reinforced concrete or steel frames can provide to be decisive in relation to structure safety. Neglecting the presence of such systems in the calculation of structures subjected to horizontal loads leads to an evaluation of stresses in the frames which is often far

from the real situation and may compromise safety. In fact, on account of the high degree of stiffness, panels do not placed symmetrically in the plan proceduce very dangerous unforeseen torsional effects. Such effects may also occur when the infills are distributed symmetrically, if there are openings for doors and windows in some of them, which cause a loss of stiffness.

The analysis is carried out utilizing the boundary element method (BEM) for the infill and opportunely dividing the frame into finite elements, so as to transform the mutual interactions of the two subsystems into stresses distributed along the boundary for the infill and into nodal actions for the frame. This makes it possible to take into account the seperation arising between the two substructures when mutual tensile stresses are involved.

At first, infills without openings are considered, using BEM with constant elements for two-dimensional problems in elasticity. Then the results are compared with those obtained using the simplified equivalent pin-jointed strut model, which is very common in literature.

Subsequently, using an analogous procedure, panels with openings are considered. For these systems, for which no satisfactory simplified models exist, the loss of stiffness in relation to the size of the opening is evaluated.

### **2.3.5 Choice of the Model**

In the previous articles several computational models are described which can be used to model and analyse infills. Of these models the first one is described in section 2.3.1 is an approximate method primarily intended for preliminary design purpose through manual calculation. The last two models are based on continuum plasticity approach in which the infill is modeled as an assemblage of several plane stress elements interacting with frame elements via special interface element. The material properties for the plane stress elements are plasticity or damage model approach. Such modeling is suitable for a detailed and micro level study of the infill panels where stress, strain, damage, cracks and failure etc. at various locations of the infill are of primary importance. Such model requires a considerable amount of computational effort due to their highly nonlinear iterative solution procedure. Such modeling is not suitable for investigating overall structural behavior of building

where infill is only a structural component. In such a situation the equivalent strut model is more suitable. The equivalent strut model proposed by Saneinejad and Hobbs (1995) is a relatively recent model capable of representing the behavior of infill satisfactorily. The model is based on an equivalent diagonal strut and uses a time rate-independent constitutive model which can be used for a static nonlinear analysis as well as time-history analysis. The same model with hysteretic formulation has been successfully used by Manders et al. 1997 for static monotonic analysis, quasi-static cyclic analysis. They have successfully verified the model by simulating experimental behavior of tested masonry infill frame subassembly. The equivalent diagonal strut model considers the entire infill panel as a single unit and takes into account only the equivalent global behavior. As a result the approach does not permit study of local effects such as frame-infill interaction within the individual infilled frame subassembly. More detailed micro modeling approaches such as the plasticity approach and the boundary element approach discussed earlier need to be used to capture the spatial and temporal variations of local conditions within the infill. However, the equivalent strut model allows for adequate evaluation of the nonlinear force deformation response of the structure and individual components under lateral load. The computed force-deformation response may be used to assess the overall structure damage and its distribution to a sufficient degree of accuracy. Thus, the proposed macro model is better suited for representing the behavior of infills in nonlinear time-history analysis of large or complex structures with multiple components particularly in cases where the focus is on evaluating the inelastic structural response. In thesis, the equivalent strut modeling, therefore, is chosen for modeling and studying the behavior of plane frames.

## 2.4 EQUIVALENT STRUT MODELLING

Considering the infilled masonry frame shown in Fig. 2.5, the maximum lateral force  $V_m$  and corresponding displacement  $u_m$  in the infill masonry panel (Saneinejad et al. 1995) are

$$V_m^+ (V_m^-) \leq A_d f'_m \cos \theta \leq \frac{vtl'}{(1 - 0.45 \tan \theta) \cos \theta} \leq \frac{0.83tl'}{\cos \theta} \quad 2.10$$

$$u_m^+(u_m^-) = \frac{\varepsilon'_m L_d}{\cos \theta} \quad 2.11$$

in which  $t$  = thickness of the infill panel;  $l'$  = lateral dimension of the infill panel;  $f'_m$  = masonry prism strength;  $\varepsilon'$  = corresponding strain;  $\theta$  = inclination of the diagonal strut;  $\nu$  = basic shear strength of masonry; and  $A_d$  and  $L_d$  = area and length of the equivalent diagonal struts respectively, calculated as

$$A_d = \frac{(1-\alpha_c)\alpha_c th \frac{\sigma_c}{f_c} + \alpha_b tl \frac{\tau_b}{f_c}}{\cos \theta} \leq 0.5 \frac{th' \frac{f_a}{f_c}}{\cos \theta} \quad 2.12$$

$$L_d = \sqrt{(1-\alpha_c)^2 h'^2 + l'^2} \quad 2.13$$

the quantities  $\alpha_c$ ,  $\alpha_b$ ,  $\sigma_c$ ,  $\tau_b$ ,  $f_a$  and  $f_c$  depends on the geometric and material properties of the frame and infill panel. These can be estimated using the formulations of the "equivalent strut model" proposed by Seneinejad et al.(1995), shown in the article 2.6. The lateral yield force  $V_y$  and displacement  $u_y$  of the infill panel may be calculated from geometry

$$V_y^+(V_y^-) = \frac{V_m - \alpha K_0 u_m}{(1-\alpha)} \quad 2.14$$

$$u_y^+(u_y^-) = \frac{V_m - \alpha K_0 u_m}{K_0(1-\alpha)} \quad 2.15$$

The initial stiffness  $K_0$  of the infill masonry panel may be estimated using the following formula(Madan et al.1997):

$$K_0 = 2(V_m/u_m) \quad 2.16$$

The parameters  $V_m$ ,  $V_y$ ,  $u_m$ ,  $u_y$ ,  $K_0$ ,  $K_l$  etc. are clearly shown in Fig.2.8. The degradation of strut stiffness from  $K_0$  to  $K_l$  was assumed to be a bilinear curve by Saneinejad and Hobbs (1995). A more rational degradation path would be a smooth curve shown by the heavy solid line in fig 2.8. However no suggestions on this form of  $V$  vs.  $u$  curve has been made so far. In this thesis the form of the curve is suggested below by equation 2.17.

In the above equation  $\alpha$  is the ratio of the final axial stiffness of the strut  $K_1$  and the initial stiffness  $K_0$ . No specific guideline is available regarding the shape of the non-linear  $V$  vs.  $u$  curve. In this study the  $V$  vs.  $u$  relation is suggested as follows

$$V = \frac{(K_0 - K_1)u}{\left[1 + \left\{\frac{K_0 - K_1}{V_0}u\right\}^2\right]^{\frac{1}{2}}} + K_1u \quad 2.17$$

in which  $K_1 = \alpha K_0$  2.18

$$V_y = \frac{V_m - \alpha K_0 u_m}{(1 - \alpha)} \quad 2.19$$

$$u_y = \frac{V_m - \alpha K_0 u_m}{K_0(1 - \alpha)} \quad 2.20$$

$$V_0 = V_y \frac{K_0 - K_1}{K_0} \quad 2.21$$

## 2.5 BEAM AND COLUMN MOMENT CAPACITY.

To find out the stiffness of equivalent strut ( $K_0$ ) it requires to determine the following properties of beam, column and joint,

$M_{pc}$  = Plastic resisting moment of column.

$M_{pb}$  = Plastic resisting moment of beam.

$M_{pj}$  = Plastic resisting moment of beam and column joint.

To determine the  $M_{pb}$ ,  $M_{pc}$  it requires to provide reinforcement in beam and column. These moments can be calculated on the basis of USD formulae,

$$M_n = A_s f_y (d - a/2)$$

$$\text{And, } \alpha = \frac{A_s f_y}{0.85 f'_c b}$$

In this thesis, it is considered 3 percent reinforcement for column and 2 percent reinforcement for beam in this analysis.  $M_{pj}$  is the sum of all  $M_{pb}$  and  $M_{pc}$  at the joint. As the column size for 7 story frame is taken as 450 mm × 450 mm, it requires 6075 mm<sup>2</sup> reinforcement. Similarly the reinforcement requires for 11 story frame is 10800 mm<sup>2</sup> as its column size is 600 mm × 600 mm. The reinforcement

required for beam is same for both 7 story and 11 story building frame. The size of beam is taken as 250 mm×600 mm, so it requires 3000 mm<sup>2</sup> reinforcement. The layout of reinforcement in beam and column are shown in fig 2.10 to 2.12.

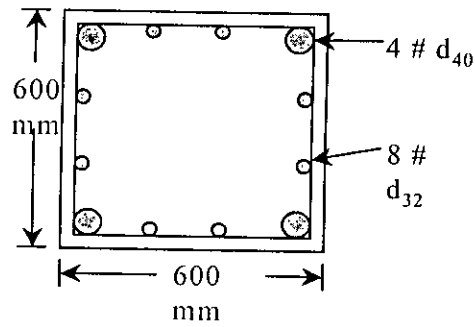


Fig 2.10 Typical layout of reinforcement in column for 11 story frame

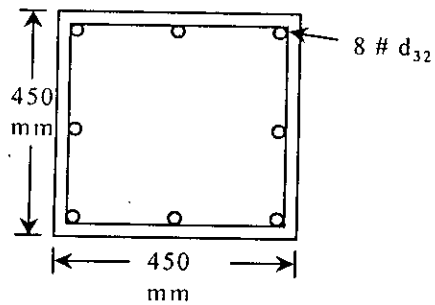


Fig 2.11 Typical layout of reinforcement in column for 7 story frame.

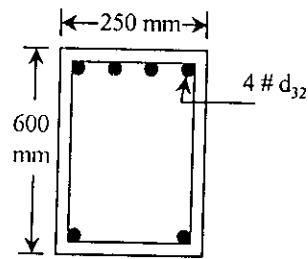


Fig 2.12 Typical layout of reinforcement in beam( at end section)

**2.6 DETERMINATION OF EQUIVALENT STRUT STIFFNESS  $K_\theta$**

The equivalent strut model proposed by Saneinejad (1995) and later modified by Madan et al.(1997) is discussed in details here. The mathematical derivation of the equivalent strut model begins with an idealized free body diagram of an infill panel and the surrounding frame as shown in Fig.2.13.

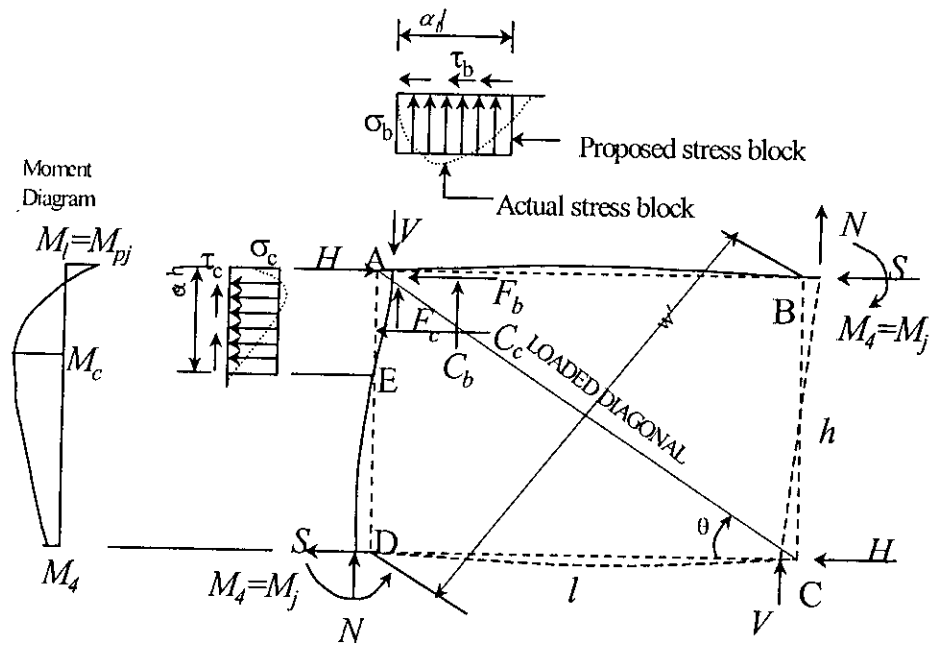


Fig 2.13 Frame forces equilibrium.

From fig 2.5 and 2.13

$$r = \frac{h}{l} < 1$$

2.22

where,  $r$  = aspect ratio of the frame.

$h$  = center to center height of beam.

$l$  = center to center length of column.

$$r' = \frac{h'}{l'} \quad 2.23$$

where  $h$  = height of infill.

$l'$  = length of infill.

$$\theta = \tan^{-1}\left(\frac{h}{l}\right) \quad 2.24$$

$$\theta' = \tan^{-1}\left(\frac{h'}{l'}\right) \quad 2.25$$

where,  $\theta$  = inclination of diagonal strut.

The effective compressive strength of infill,  $f_c$  can be calculated by

$$f_c = 0.6\phi f_m' \quad 2.26$$

where,  $\phi$  is a constant and its value is 0.65.

$f_m'$  = compressive strength of masonry.

The length of the proposed stress blocks (Fig2.13) may not exceed 0.4 times the corresponding infill dimensions

$$\alpha_c h \leq 0.4h' \quad 2.27$$

$$\alpha_b l \leq 0.4l' \quad 2.28$$

where  $\alpha$  = normalized length of contact; and subscripts  $c$  and  $b$  designate column and beam, respectively.

Frame/infill interaction is associated with shear forces that may be evaluated closely by the following:

$$F_c = \mu r^2 C_c \quad 2.29$$

$$F_b = \mu C_b \quad 2.30$$

where  $C$  and  $F$  = frame/infill contact normal and shear forces ( Fig.2.13) and  $\mu$  = coefficient of friction of the frame/infill interface. At the peak load

$$M_A = M_C = M_{pj} \quad 2.31$$

where  $M_A$  and  $M_C$  = bending moments at loaded corners (points A and C in Fig.2.13); and  $M_{pj}$  = least of the beam, the column, and their connection plastic resisting moment, called the joint plastic resisting moment.

$$M_D = M_B = M_j < M_{pj} \quad 2.32$$

$$M_c = \beta_c M_{pc} \quad 2.33$$

$$M_b = \beta_b M_{pb} \quad 2.34$$

where  $M_B$  and  $M_D$  = bending moments at the unloaded corners (Fig.2.13) and  $M_j$  represents either of these values. Also  $M_c$  and  $M_b$  are maximum intermediate elastic moment of column and beam.

$$\beta_c \leq \beta_0 = 0.2 \quad 2.35$$

$$\beta_b \leq \beta_0 = 0.2 \quad 2.36$$

where  $\beta_0$  = nominal, or rather upper-bound, value of the reduction factors,  $\beta$ .

Let  $h' = h$  and  $l' = l$

Frame forces equilibrium requires the following:

$$V = H \tan \theta \quad 2.37$$

$$H = C_c + F_b + 2S \quad 2.38$$

$$V = C_b + F_c + 2N \quad 2.39$$

Rotational equilibrium of the infill requires the following:

$$C_c \left( \frac{h}{2} - \alpha_c \frac{h}{2} \right) - F_c \frac{l}{2} - C_b \left( \frac{l}{2} - \alpha_b \frac{l}{2} \right) + F_b \frac{h}{2} = 0 \quad 2.40$$

$$\text{where } C_c = \sigma_c t \alpha_c h,$$

$$C_b = \sigma_b t \alpha_b l,$$

$$F_c = \tau_c t \alpha_c h \text{ and}$$

$$F_b = \tau_b t \alpha_b l.$$

$H$  and  $V$  = horizontal and vertical components of the external forces;  $S$  and  $N$  = shear and axial forces, respectively, over the uncontacted length of the column;  $\sigma$  and  $\tau$  = proposed uniform frame/infill contact normal and shear forces,  $\theta$  = sloping angle of the infill diagonal. Taking the static moment of the forces acting on the column and beam about point A:

$$S = -0.5 \sigma_c t \alpha_c^2 h + \frac{(M_{pj} + M_j)}{h} \quad 2.41$$

$$N = -0.5\sigma_b t \alpha_b^2 l + \frac{(M_{pj} + M_j)}{l} \quad 2.42$$

Substituting for contact forces,  $C_c$  and  $F_b$ , and also column shear force,  $S$  into 2.38 leads to the collapse load, as follows:

$$H = \sigma_c t (1 - \alpha_c) \alpha_c h + \tau_b t \alpha_b l + 2 \frac{(M_{pj} + M_j)}{h} \quad 2.43$$

At peak load, the infill is subjected to failure resulting from combined normal and shear stresses acting on the contacted surfaces in the loaded corners. The well known Tresca hexagonal yield criterion, described by Chen (1982), is mathematically convenient for this combination, and is given by

$$\sigma^2 + 3\tau^2 = f_c^2 \quad 2.44$$

where  $f_c$  = effective compressive strength of the infill.

Assuming rectangular stress blocks, as shown in Fig. 2.13, can be written also in terms of the contact stresses, as follows:

$$\tau_c = \mu \sigma_c \quad 2.45$$

$$\tau_b = \mu \sigma_b \quad 2.46$$

Combining 2.44, 2.45 and 2.46 and solving for the contact stresses leads to the nominal (upper-bound) values of the contact normal stresses

$$\sigma_{c0} = \frac{f_c}{\sqrt{1 + 3\mu^2 r^4}}; \quad 2.47$$

$$\sigma_{b0} = \frac{f_c}{\sqrt{1 + 3\mu^2}} \quad 2.48$$

Taking the static moment of the forces acting on the column along EA gives the following:

$$M_{pj} + M_c - 0.5(\alpha_c h)^2 \sigma_c t = 0 \quad 2.49$$

A similar relation can be written for the beam as follows:

$$M_{pj} + M_b - 0.5(\alpha_b l)^2 \sigma_b t = 0 \quad 2.50$$

Substituting for  $M_c$  and  $M_b$  from 2.33 and 2.34 into 2.49 and 2.50 and solving for the contact lengths, leads to the following:

$$\alpha_c h = \sqrt{\frac{2M_{pj} + 2\beta_c M_{pc}}{\sigma_c t}}; \quad 2.51$$

$$\alpha_b l = \sqrt{\frac{2M_{pj} + 2\beta_b M_{pb}}{\sigma_b t}} \quad 2.52$$

Either  $\beta_c$  or  $\beta_b$  would approach their upper-bound value,  $\beta_0 = 0.2$ , when the contact surface in question develops the corresponding nominal normal stress. Substituting for these nominal values and combining with 2.27 and 2.28 leads to the following:

$$\alpha_c h = \sqrt{\frac{2M_{pj} + 2\beta_0 M_{pc}}{\sigma_{c0} t}} \leq 0.4h'; \quad 2.53$$

$$\alpha_b l = \sqrt{\frac{2M_{pj} + 2\beta_0 M_{pb}}{\sigma_{b0} t}} \leq 0.4l' \quad 2.54$$

Substituting for the contact forces into 2.40 gives the following:

$$\sigma_b \alpha_b (1 - \alpha_b - \mu r) = r^2 \sigma_c \alpha_c (1 - \alpha_c - \mu r) \quad 2.55$$

This relation would be satisfied only with the real contact stresses, generated from the nominal contact stresses, (2.47 and 2.48), as follows:

$$\text{If } A_c > A_b, \text{ then } \sigma_b = \sigma_{b0} \text{ and } \sigma_c = \sigma_{c0}(A_b / A_c) \quad 2.56$$

$$\text{If } A_b > A_c, \text{ then } \sigma_c = \sigma_{c0} \text{ and } \sigma_b = \sigma_{b0}(A_c / A_b) \quad 2.57$$

Where

$$A_c = r^2 \sigma_{c0} \alpha_c (1 - \alpha_c - \mu r) \quad 2.58(a)$$

$$A_b = \sigma_{b0} \alpha_b (1 - \alpha_b - \mu r) \quad 2.58(b)$$

The actual compressive strength of masonry depends on the direction of stresses and it can be found by following

$$f_a = f_c \left[ 1 - \left( \frac{L_d}{40t} \right)^2 \right] \quad 2.59$$

The effective length of diagonal strut

$$L_d = \sqrt{(1 - \alpha_c)^2 h'^2 + l'^2} \quad 2.60$$

where  $L_d$  is not greater than  $40t$  and  $f_c$  is effective compressive strength of masonry.

The cross sectional area of the diagonal strut for effective compressive strength  $f_c$  is

$$A_d = \frac{(1 - \alpha_c) \alpha_c t h \frac{\sigma_c}{f_c} + \alpha_b t l \frac{\tau_b}{f_c}}{\cos \theta} \leq 0.5 \frac{t h' \frac{f_a}{f_c}}{\cos \theta} \quad 2.61$$

The maximum lateral force  $V_m$  and corresponding displacement  $u_m$  in the infill masonry panel are

$$V_m^+ (V_m^-) \leq A_d f'_m \cos \theta \leq \frac{v l l'}{(1 - 0.45 \tan \theta) \cos \theta} \leq \frac{0.83 l l'}{\cos \theta} \quad 2.62$$

$$u_m^+ (u_m^-) = \frac{\varepsilon'_m L_d}{\cos \theta} \quad 2.63$$

Finally, the initial stiffness  $K_0$  of the infill masonry panel may be estimated using the equation 2.16.

### Example of determining $K_0$ for 11 story

The column is 600 mm x 600 mm and the beam is 250 mm x 600 mm.

Equations 2.22 to 2.64 are used to determine  $K_0$

$$\phi = 0.65, f_m = 12 \text{ Mpa}, \mu = 0.65, \beta_0 = 0.2, \varepsilon'_m = 0.002, v = 6 \text{ Mpa}$$

| $t$    | $h$     | $h'$    | $L$     | $l'$    | $\phi$ | $\mu$ |
|--------|---------|---------|---------|---------|--------|-------|
| 150 mm | 3000 mm | 2400 mm | 4500 mm | 3900 mm | 0.65   | 0.65  |
| 250 mm | 3000 mm | 2400 mm | 4500 mm | 3900 mm | 0.65   | 0.65  |

| $t$    | $f'_m$    | $\beta_o$ | $M_{pj}$       | $M_{pc}$       | $M_{pb}$       | $r$    | $r'$   |
|--------|-----------|-----------|----------------|----------------|----------------|--------|--------|
| 150 mm | 12<br>MPa | 0.2       | 5.46e8<br>N-mm | 7.90e8<br>N-mm | 5.46e8<br>N-mm | 0.6667 | 0.6154 |
| 250 mm | 12<br>MPa | 0.2       | 5.46e8<br>N-mm | 7.90e8<br>N-mm | 5.46e8<br>N-mm | 0.6667 | 0.6154 |

| $t$    | $\theta$           | $\theta'$          | $f_c$       | $\sigma_{c0}$               | $\sigma_{b0}$               | $\alpha_c$ | $\alpha_b$ |
|--------|--------------------|--------------------|-------------|-----------------------------|-----------------------------|------------|------------|
| 150 mm | 33.69 <sup>0</sup> | 31.60 <sup>0</sup> | 4.68<br>MPa | 4.1853<br>N/mm <sup>2</sup> | 3.1079<br>N/mm <sup>2</sup> | 0.32       | 0.3466     |
| 250 mm | 33.69 <sup>0</sup> | 31.60 <sup>0</sup> | 4.68<br>MPa | 4.1853<br>N/mm <sup>2</sup> | 3.1079<br>N/mm <sup>2</sup> | 0.32       | 0.2885     |

| $t$    | $A_c$                      | $A_b$                       | $\sigma_c$                  | $\sigma_b$                  | $\tau_b$                    | $\tau_c$                    | $L_d$         |
|--------|----------------------------|-----------------------------|-----------------------------|-----------------------------|-----------------------------|-----------------------------|---------------|
| 150 mm | 0.14826<br>mm <sup>2</sup> | 0.237032<br>mm <sup>2</sup> | 4.1853<br>N/mm <sup>2</sup> | 1.9251<br>N/mm <sup>2</sup> | 1.2513<br>N/mm <sup>2</sup> | 1.2091<br>N/mm <sup>2</sup> | 4227.69<br>mm |
| 250 mm | 0.14826<br>mm <sup>2</sup> | 0.249412<br>mm <sup>2</sup> | 4.1853<br>N/mm <sup>2</sup> | 1.8296<br>N/mm <sup>2</sup> | 1.1892<br>N/mm <sup>2</sup> | 1.2091<br>N/mm <sup>2</sup> | 4227.69<br>mm |

| $t$   | $f_a$      | $A_d$                     | $u_m$     | $V_m$      | $K_o$          |
|-------|------------|---------------------------|-----------|------------|----------------|
| 150mm | 2.3564 MPa | 108927<br>mm <sup>2</sup> | 10.162 mm | 583558.5 N | 114850<br>N/mm |
| 250mm | 3.8435 MPa | 226260<br>mm <sup>2</sup> | 10.162 mm | 972597 N   | 191416<br>N/mm |

---

**CHAPTER 3**

**COMPUTATIONAL MODELING OF INFILLED FRAMES**

---

### 3.1 INTRODUCTION

The computational modeling of infilled frames has been described briefly in this chapter. The finite element modeling of infilled frames including modeling of beams and columns, modeling of infill, calculation of lateral load according to BNBC, developing of finite element mesh with or without infill has also been described in this chapter. Selection of element type of modeling frames including beam, column and nonlinear spring also described. The nonlinear spring element is used to represent the diagonal strut of infill. The various obstacles faced during modeling, material behavior used and details of finite element meshing were described in detail.

### 3.2 THE FINITE ELEMENT PACKAGES

A number of good finite element analysis computer packages are available in the civil engineering field. They vary in degree of complexity, usability and versatility. The names of such packages are :

|            |        |       |        |        |
|------------|--------|-------|--------|--------|
| Micro Feap | ABQUAS | STAAD | SAP 90 | MARC   |
| FEMSKI     | ADINA  | ANSYS | DIANA  | STRAND |

Some of these programs are intended for a special type of structure. For example Micro Feap P1 is developed for the analysis of plane frames and truss while Micro Feap P2 is for the analysis of slab and roof system. Of these, here the package ANSYS has been for its relative ease of use, detailed documentation, flexibility and vastness of its capabilities. The version of ANSYS has been used was the special Student's Edition Version ANSYS 5.4.

ANSYS is one of the most powerful and versatile packages available for finite element structural analysis. The term structural implies not only civil engineering structures such as bridges and buildings, but also naval, aeronautical, and

mechanical structures such as ship hulls, aircraft bodies, and machine housings, as well as mechanical components such as pistons, machine parts, and tools. The seven types of structural analysis available in the ANSYS family of products :

- 1) Static analysis
- 2) Modal analysis
- 3) Harmonic analysis
- 4) Transient dynamic analysis
- 5) Spectrum analysis
- 6) Buckling analysis
- 7) Explicit dynamic analysis

The primary unknowns ( nodal degrees of freedom ) calculated in a structural analysis are displacements. Other quantities, such as strains, stresses, and reaction forces, are then derived from the nodal displacements. Especially its graphical representations are very distinct. Finally the ANSYS program is user friendly. It has a comprehensive graphical user interface ( GUI ) that gives user easy, interactive access to program functions, commands, documentations and reference material. An intuitive menu system helps user to navigate through the ANSYS program. User can input data using a mouse, a keyboard or a combination of both.

### **3.3 FINITE ELEMENT MODELING OF INFILLED FRAMES**

Reinforced concrete frame is a composite type of structure. Reinforced cement concrete, speaking in very common sense, is a mass of hardened concrete with steel reinforcement embedded within it. In usual practice reinforced cement concrete frames is assumed as a homogeneous and isotropic material. For simplicity in analysis 3-D elastic beam of ANSYS has been selected to model the RC frame. The concrete properties are used for 3-D elastic beam. Several past studies on RC frames and ACI recommends that if only concrete properties are used for 3-D elastic beam element, the analysis will give sufficiently accurate result.

Infill is provided in RC frame for increasing stability and reducing displacement against lateral load. The infill acts as a diagonal strut against lateral

load according to equivalent strut method. This method is described in Art. 2.3.2. Since the tensile strength of masonry is negligible, so only compressive diagonal strut is liable to resist the lateral load. In this analysis we select nonlinear spring element to represent the equivalent diagonal strut. The values  $u$  versus  $V$  of nonlinear  $u$ - $V$  curve are used as real constants.

### 3.3.1 Modeling of Beams and Columns

The beams and columns of the frame were represented by the same element Beam4 3-D elastic beam. It is basically a two noded frame element having three displacements and three rotational degrees of freedom at each node. All the beams and columns elements of the frame are modeled by the base element Beam4 3-D elastic beam owing to simplicity. All beams and columns element are rectangular in shape. Here the base elements of ANSYS package are discussed in details .

#### Beam4 3-D elastic beam

Beam4 is a uniaxial element with tension, compression, torsion and bending capabilities. The element has six degrees of freedom at each node, translation in the nodal  $x$  ,  $y$  and  $z$  directions and rotations about the nodal  $x$ ,  $y$  and  $z$  axes. Fig 3.1 shows a typical shape of beam4 3-D elastic beam.

#### Input data

The geometry, node locations, and co-ordinate systems for this element are shown in fig 3.1. The element is defined by two or three nodes, the cross sectional area, two area moment of inertia ( $I_{zz}$  and  $I_{yy}$ ), two thickness ( $TK_y$  and  $TK_z$ ), and the material properties.

A summary of the element input is given below in table 3.1

| Beam4 Input Summary |   |
|---------------------|---|
| Element Name        | BEAM4                                     |
| Nodes               | I, J, K (K orientation node is optional)  |
| Degrees of Freedom  | $U_x, U_y, U_z, ROT_x, ROT_y$ and $ROT_z$ |
| Real Constants      | AREA, $I_{zz}, I_{yy}, TK_y, TK_z$        |
| Material Properties | $E_x$ , Density and Poisson's Ratio       |

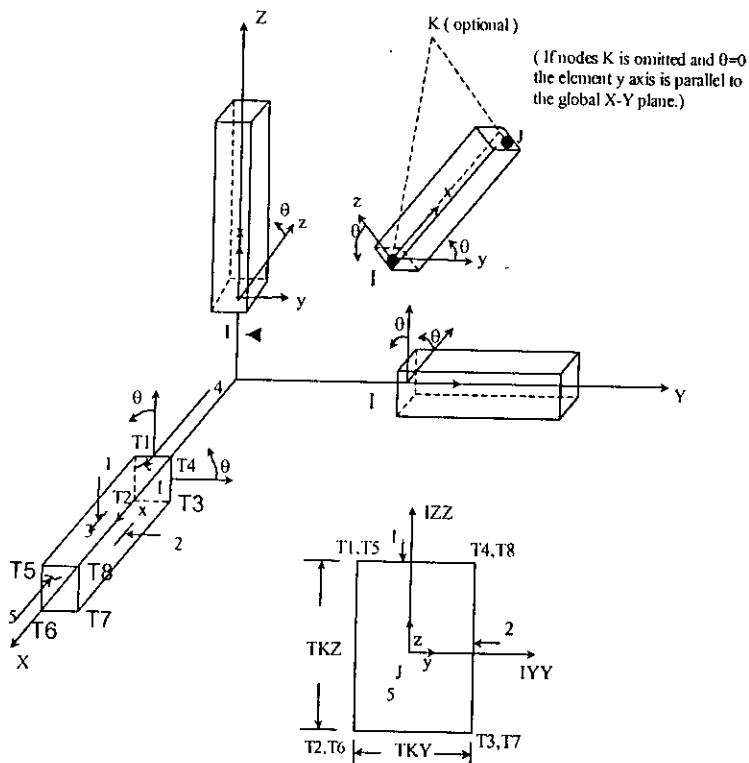


Fig 3.1 BEAM4 3-D Elastic Beam

**Output data**

The solution output associated with the element is in two forms: 1) nodal displacements included in the overall nodal solutions. 2) the elemental solutions. By

plotting result from general postprocessor we can see the deformed shape of nodes and elements. From list result of general post processor we can get nodal translation in the X, Y and Z directions and rotation about X, Y and Z directions. As our applied force lateral in X direction, so the displacement of node in Z and rotation in the X and Y axis are zero. From the list result element solutions we can get moments, force in X, Y and Z directions for various elements. The main purpose of this analysis is to calculate translations of nodes in the X direction for lateral load.

### **Assumptions and restrictions**

The beam must not have a zero length or area. The moments of inertia, however, may be zero if large deflections are not used. But in this analysis the moment of inertia is not zero. The beam can have any cross sectional shape for which the moments of inertia can be computed.

### **3.3.2 Modeling of infill**

One of the most remarkable feature of our FE modeling is modeling the infill. ANSYS element COMBIN 39 is used to model the infill as diagonal strut. It is basically a pin ended truss element with non-linear capabilities. We will first describe the element that is used to simulate the infill characteristics in the finite element model.

### **COMBIN39 Nonlinear Spring**

COMBIN39 is a unidirectional element with nonlinear generalized force-deflection capability that can be used in any analysis. The element has longitudinal or torsional capability in one, two, or three dimensional applications. The longitudinal option is a uniaxial tension-compression element with upto three degrees of freedom at each node: translations in the nodal x, y and z directions. No bending or torsion is considered. The torsional option is a purely rotational element with three degrees of freedom at each node: rotations about the nodal x, y and z axes. No bending or axial loads are considered. The element has large displacement capability for which there can be two or three degrees of freedom at each node. Fig 3.2 shows a typical COMBIN39 nonlinear spring.

### Input Data

The geometry, node locations, and the coordinate system for this element are shown in fig 3.2. The element is defined by two node points and a generalized force-deflection curve. The points on this curve (  $D_1$  ,  $F_1$  , etc. ) represent force ( or moment) versus relative translation ( or rotation ) for structural analysis. The force-

deflection curve should be input such that deflections are increasing from the third (compression ) to the first ( tension ) quadrants.

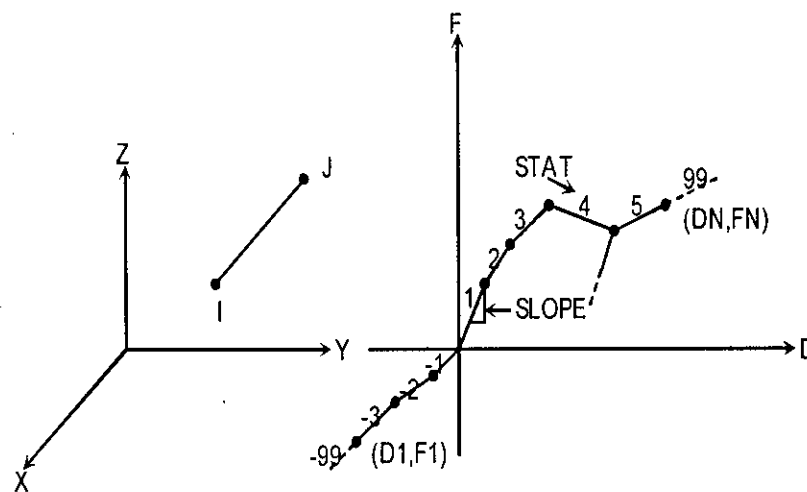


Fig 3.2 COMBIN39 Nonlinear spring

A summary of element input is given in table 3.2

| COMBIN39 Input Summary |   |
|------------------------|---|
| Element name           | COMBIN39                                    |
| Nodes                  | I , J                                       |
| Degrees of Freedom     | $U_x, U_y, U_z, ROT_x, ROT_y, ROT_z$        |
| Real Constants         | $D_1, F_1, D_2, F_2, \dots, D_{19}, F_{19}$ |
| Material Properties    | None  |

### **Output data**

The solution output associated with the element is in two forms: 1) nodal degree of freedom results included in the overall nodal solution, and 2) additional element output solution. We can get nodal translation and rotation in the X, Y and Z direction, similarly element force, moment in the X, Y and Z direction from general post processor. The only nodal translation in the X direction is required for this analysis.

### **Assumptions and restriction**

The element assumes only a one-dimensional action. Nodes I and J may be anywhere in space. The element is defined such that a positive displacement of node J relative to node I tends to put the element in tension.

The element is nonlinear and requires an iterative solution. The nonlinear behavior of the element operates only in the static and nonlinear transient dynamic analysis. As the most nonlinear elements, loading and unloading should occur gradually. When the element is also nonconservative, loads should be applied along the actual load history path and in the proper sequence.

## **3.4 LOADS**

In the present investigation, we have chosen wind as the source of lateral loading on the building frame. The minimum design wind load on buildings and components thereof shall be determined based on the velocity of wind, the shape and size of the building and the terrain exposure condition of the site as set forth by the provisions of Bangladesh National Building Code (BNBC, 1993).

Article 2.4 from BNBC (1993) is used for the calculation of design wind loads for the buildings in this thesis. The design wind load shall include the effects of the sustained wind velocity component and the fluctuating component due to gusts.

**Determination of design wind loads**

The plan and elevation of the 7<sup>th</sup> and 11<sup>th</sup> story building is shown in Figs.3.3, 3.4 and 3.5. As the structure is assumed to exist in Dhaka, the basic wind speed  $V_b = 210$  Km/h.

From fig 3.5

$$L/B = 13500/32500 = 0.4154$$

For 7 story  $h/B = 21650/32500 = 0.666$ , and for 11 story  $h/B = 33650/32500 = 1.035$

Overall pressure coefficient,

$$C_p \text{ for 7 story} = 1.445$$

$$C_p \text{ for 11 story} = 1.4586$$

$$C_G \text{ for 7 story} = 1.356 \text{ and}$$

$$C_G \text{ For 11 story} = 1.29$$

Sustained wind pressure,

$$q_z = C_c C_I C_z V_b^2 \quad 3.1$$

Where,

$$V_b = \text{Basic wind speed} = 210 \text{ Km/h}$$

$$C_c = \text{Velocity to pressure conversion co-efficient} = 47.2 \times 10^{-6}$$

$$C_I = \text{Structural importance co-efficient} = 1.00$$

$$C_z = \text{Combined height and exposure co-efficient}$$

From equation (3.1) sustained wind pressure.

$$q_z = (47.2 \times 10^{-6}) \times (1.00) \times C_z \times (210)^2$$

$$q_z = (2.082) \times C_z \quad 3.2$$

Design wind pressure,

$$p_z = C_G C_p q_z$$

Where,  $C_G =$  Gust response factor and

$C_p =$  overall pressure co-efficient.

**Design wind load for 7 story building frame**

| Height in<br>Metre | $C_z$ | $q_z = (2.082) \times C_z$ | $p_z = C_G C_p q_z$<br>in KN/m <sup>2</sup> | Design wind<br>load ( N ) |
|--------------------|-------|----------------------------|---|---------------------------|
| 3.65               | 0.368 | 0.7662                     | 1.501                                       | $32.25 \times 10^3$       |
| 6.65               | 0.433 | 0.902                      | 1.767                                       | $34.57 \times 10^3$       |
| 9.65               | 0.512 | 1.07                       | 2.097                                       | $40.94 \times 10^3$       |
| 12.65              | 0.580 | 1.21                       | 2.371                                       | $46.28 \times 10^3$       |
| 15.65              | 0.636 | 1.33                       | 2.606                                       | $50.92 \times 10^3$       |
| 18.65              | 0.687 | 1.43                       | 2.802                                       | $55.05 \times 10^3$       |
| 21.65              | 0.735 | 1.53                       | 2.998                                       | $29.43 \times 10^3$       |

**Design wind load for 11 story building frame**

| Height in<br>Metre | $C_z$  | $q_z = (2.082) \times C_z$ | $p_z = C_G C_p q_z$<br>in KN/m <sup>2</sup> | Design wind<br>load ( N ) |
|--------------------|--------|----------------------------|---|---------------------------|
| 3.65               | 0.368  | 0.7662                     | 1.442                                       | $31.58 \times 10^3$       |
| 6.65               | 0.433  | 0.902                      | 1.695                                       | $33.88 \times 10^3$       |
| 9.65               | 0.512  | 1.07                       | 2.004                                       | $40.16 \times 10^3$       |
| 12.65              | 0.580  | 1.21                       | 2.271                                       | $45.33 \times 10^3$       |
| 15.65              | 0.636  | 1.33                       | 2.491                                       | $49.88 \times 10^3$       |
| 18.65              | 0.687  | 1.43                       | 2.691                                       | $53.91 \times 10^3$       |
| 21.65              | 0.735  | 1.53                       | 2.879                                       | $57.65 \times 10^3$       |
| 24.65              | 0.777  | 1.62                       | 3.043                                       | $60.04 \times 10^3$       |
| 27.65              | 0.8185 | 1.71                       | 3.205                                       | $64.25 \times 10^3$       |
| 30.65              | 0.857  | 1.78                       | 3.336                                       | $67.26 \times 10^3$       |
| 33.65              | 0.892  | 1.86                       | 3.493                                       | $33.24 \times 10^3$       |

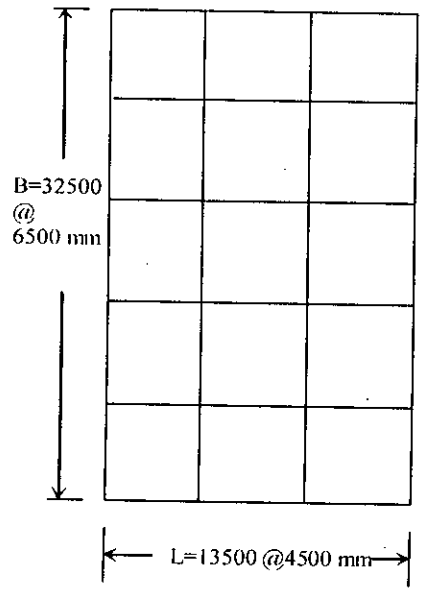


Fig 3.3 Plan of structure (7 and 11 story)

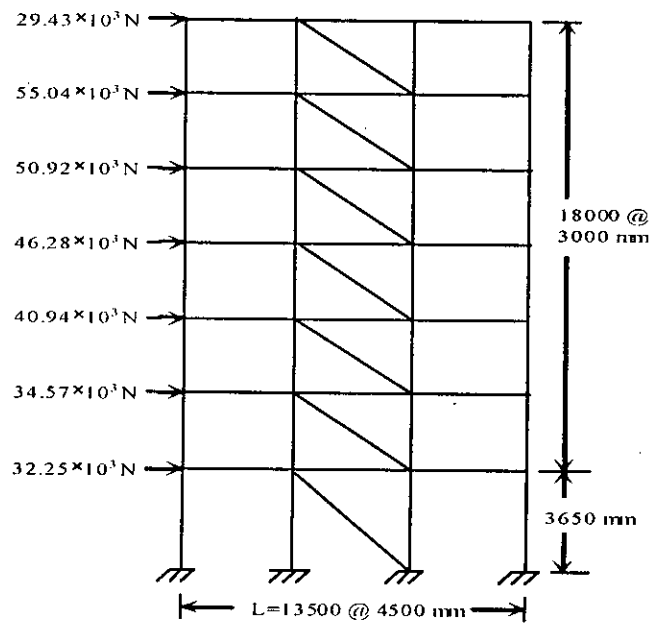


Fig.3.4. Elevation of 7 story frame

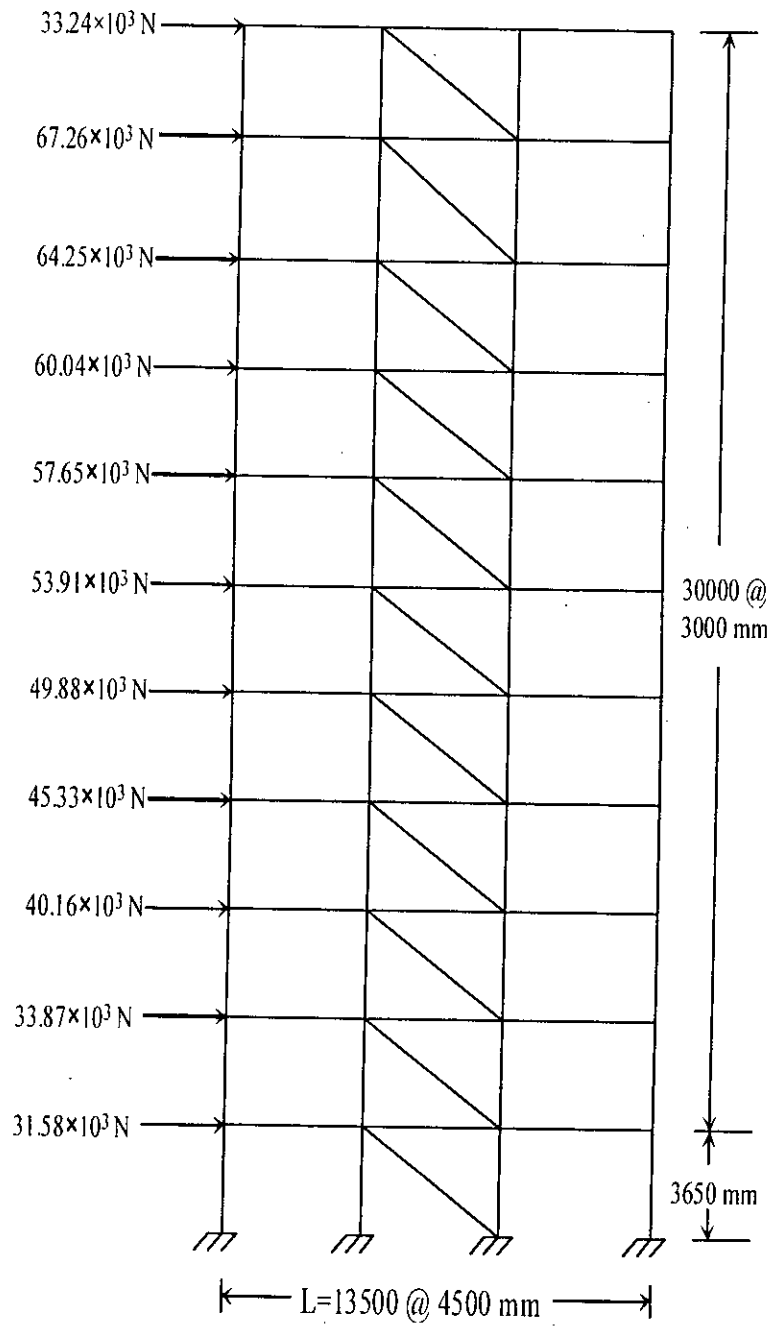


Fig 3.5 Elevation of 11 story frame

### 3.5 DEVELOPING THE FINITE ELEMENT MESH

In this thesis we are studying framed structure with infill. Therefore frame elements are used in modeling the framed structure and equivalent strut is used for representing the infill. These elements are described in article 3.3. In this thesis there are two types of structures are studied namely 7 storied frame and 11 storied frame with and without infill. Each of the frame has three equal spans. The basic dimension of the frames are described in article 3.4.

In the 1<sup>st</sup> step of developing the mesh nodes are created by displayed work plane setting in ANSYS. The spacing of these nodes are in accordance with the span and height of the floors. For each floor four nodes are required. Therefore the 7 story frame consists of 32 nodes including the four ground floor nodes. Each floor has 3 beams and 4 columns, that is 7 frame elements are required for each floor. Thus 49 elements are required for 7 story building frame. Additionally 7 strut elements are used to model the infill in the central span. Similarly for 11 story building frame consists of 48 nodes. 77 frame elements are required for 11 story building frame. Additionally 11 strut elements are used to model the infill in the central span.

These frames with or without infill for 7 story are shown in Fig 3.6 and Fig 3.7 and for 11 story in Fig 3.8 and Fig 3.9.

An important part of this analysis is to apply loads in the frame. These loads are already calculated in article 3.4 according to BNBC. These loads are shown in Fig 3.4 for 7 story building frame and Fig 3.5 for 11 story building frame. The same loads are applied on the finite element mesh along the left side nodes of the frame.

### 3.6 TYPICAL ANALYSIS RESULTS.

The descriptions of beam and column for the frame were given in chapter 2 article 2.5. These descriptions are used here for frame analysis. The input parameter of column, beam and strut element for 7 story and 11 story frame are as follows:

**Column input parameters :**

7 story input parameters given in table 3.4 below

|  |                            |
|--|----------------------------|
| Column size                                | 450 mm × 450 mm            |
| Cross-sectional area , AREA                | 202500 mm <sup>2</sup>     |
| Area moment of inertia , I <sub>zz</sub>   | 3417187584 mm <sup>4</sup> |
| Area moment of inertia , I <sub>yy</sub>   | 3417187584 mm <sup>4</sup> |
| Thickness along Z axis , TK <sub>z</sub>   | 450 mm                     |
| Thickness along Y axis , TK <sub>y</sub>   | 450 mm                     |
| Poisson's ratio (minor) , Nu <sub>xy</sub> | 0.15                       |
| Young's modulus , E <sub>x</sub>           | 24855.19 N/mm <sup>2</sup> |

11 story input parameters given in table 3.5 below

|  |                             |
|--|-----------------------------|
| Column size                                | 600 mm × 600 mm             |
| Cross-sectional area , AREA                | 360000 mm <sup>2</sup>      |
| Area moment of inertia , I <sub>zz</sub>   | 10800000000 mm <sup>4</sup> |
| Area moment of inertia , I <sub>yy</sub>   | 10800000000 mm <sup>4</sup> |
| Thickness along Z axis , TK <sub>z</sub>   | 600 mm                      |
| Thickness along Y axis , TK <sub>y</sub>   | 600 mm                      |
| Poisson's ratio (minor) , Nu <sub>xy</sub> | 0.15                        |
| Young's modulus , E <sub>x</sub>           | 24855.19 N/mm <sup>2</sup>  |

**Beam input parameters**

Table 3.6 both for 7 story and 11 story frame

|  |                           |
|--|---------------------------|
| Beam size                                  | 250 mm × 600 mm           |
| Cross-sectional area , AREA                | 150000 mm <sup>2</sup>    |
| Area moment of inertia , I <sub>zz</sub>   | 449999744 mm <sup>4</sup> |
| Area moment of inertia , I <sub>yy</sub>   | 781249984 mm <sup>4</sup> |
| Thickness along Z axis , TK <sub>z</sub>   | 250 mm                    |
| Thickness along Y axis , TK <sub>y</sub>   | 600 mm                    |
| Poisson's ratio (minor) , Nu <sub>xy</sub> | 0.15                      |

|                         |                            |
|-------------------------|----------------------------|
| Young's modulus , $E_x$ | 24855.19 N/mm <sup>2</sup> |
|-------------------------|----------------------------|

### Strut input parameters ( COMBIN39-Nonlinear spring )

A set of values of lateral force  $V$  and deflection  $u$  of nonlinear  $u-V$  curve are used as input parameters for COMBIN39-Nonlinear spring.

### Example of determining input parameters for COMBIN39-nonlinear spring

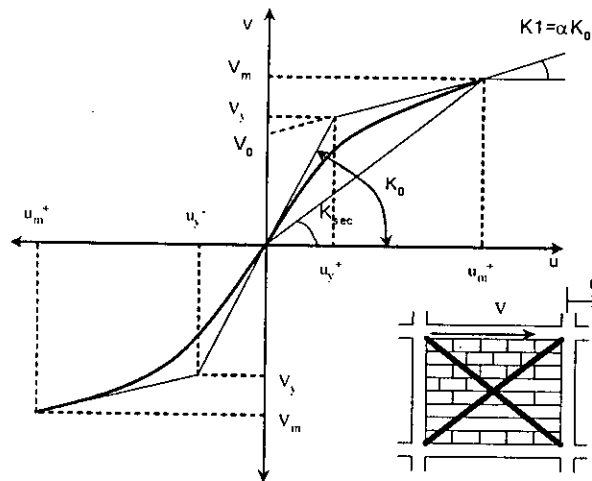


Fig.2.8 ( repeated ) Non linear  $u-V$  curve for masonry infill panel

$K_0$ ,  $V_m$  and  $u_m$  are found using the same procedure as described in article 2.6.

#### For 7 story (infill thickness 150 mm)

Here  $K_0=115477$  N/mm

$$V_m=606003 \text{ N}$$

$$u_m=10.49 \text{ mm}$$

To get a nonlinear  $u-V$  curve the values of  $u_m$  are multiplied by 0.05, 0.10, ----, 0.85 etc.

Then corresponding  $V$  values are found as follows:

#### For example

$$u_m=10.49 \text{ mm}$$

$$0.05 \times u_m=0.5245 \text{ mm}$$

$$0.10 \times u_m=1.049 \text{ mm}$$

-----

-----

$$0.85 \times u_m=8.91 \text{ mm}$$

Now, the procedure of calculating  $V$  value of corresponding  $u$  value of 0.5245

$$K_1 = \alpha K_0 \quad (\text{assuming } \alpha = 0.10)$$

$$= 0.10 \times 115477$$

$$= 11547.7 \text{ N/mm}$$

$$V_y = \frac{V_m - \alpha K_0 u_m}{(1 - \alpha)}$$

$$= \frac{606003 - 0.10 \times 115477 \times 10.49}{1 - 0.10}$$

$$= 538741 \text{ N}$$

$$V_0 = V_y \frac{K_0 - K_1}{K_0}$$

$$= 538741 \frac{115477 - 11547.7}{115477}$$

$$= 484866 \text{ N}$$

$$V = \frac{(K_0 - K_1)u}{\left[1 + \left\{\frac{K_0 - K_1}{V_0}u\right\}^2\right]^{\frac{1}{2}}} + K_1 u$$

$$= \frac{(115477 - 11547.7) \times 0.5245}{\left[1 + \left\{\frac{115477 - 11547.7}{484866} \times 0.5245\right\}^2\right]^{\frac{1}{2}}} + 11547.7 \times 0.5245$$

$$= \frac{54510.91}{1.006299} + 6056.76$$

$$= 60226 \text{ N}$$

Similarly for other values of  $V$  were calculated for corresponding values of  $u$  and tables were prepared with input parameters of COMBIN 39-nonlinear spring.

Table 3.7.1 An example of input parameter for 7 story infill(150 mm thick )

| u (mm) | V (N)    |
|--------|----------|
| - 8.92 | - 532638 |
| - 7.87 | - 507971 |
| - 6.82 | - 478975 |
| - 5.77 | - 443736 |
| - 4.72 | - 399469 |
| - 3.67 | - 342361 |
| - 2.62 | - 267980 |
| - 1.57 | - 173209 |
| - 0.52 | - 60258  |
| 0      | 0        |
| 0.52   | 60258    |
| 1.57   | 173209   |
| 2.62   | 267980   |
| 3.67   | 342361   |
| 4.72   | 399469   |
| 5.77   | 443736   |
| 6.82   | 478975   |
| 7.87   | 507971   |
| 8.92   | 532638   |

Table 3.7.2 An example of input parameter for 7 story infill (250 mm thick )

| u(mm)  | V(N)     |
|--------|----------|
| - 8.97 | - 887730 |
| - 7.92 | - 846619 |
| - 6.86 | - 798292 |
| - 5.81 | - 739560 |
| - 4.75 | - 665783 |
| - 3.69 | - 570603 |

|        |          |
|--------|----------|
| - 2.64 | - 446633 |
| - 1.58 | - 288682 |
| - 0.52 | - 100430 |
| 0      | 0        |
| 0.52   | 100430   |
| 1.58   | 288682   |
| 2.64   | 446633   |
| 3.69   | 570603   |
| 4.75   | 665783   |
| 5.81   | 739560   |
| 6.86   | 798292   |
| 7.92   | 846619   |
| 8.97   | 887730   |

Table 3.8.1 An example of input parameter for 11 story infill (150 mm thick )

| u(mm)  | V(N)     |
|--------|----------|
| - 8.63 | - 512911 |
| - 7.62 | - 489158 |
| - 6.60 | - 461235 |
| - 5.58 | - 427301 |
| - 4.57 | - 384674 |
| - 3.55 | - 329681 |
| - 2.54 | - 258054 |
| - 1.52 | - 166794 |
| - 0.50 | - 58026  |
| 0      | 0        |
| 0.50   | 58026    |
| 1.52   | 166794   |
| 2.54   | 258054   |
| 3.55   | 329681   |

|      |        |
|------|--------|
| 4.57 | 384674 |
| 5.58 | 427301 |
| 6.60 | 461235 |
| 7.62 | 489158 |
| 8.63 | 512911 |

Table 3.8.2 An example of input parameter for 11 story infill (250 mm thick )

| u(mm)  | V(N)     |
|--------|----------|
| - 8.63 | - 854852 |
| -7.62  | - 815263 |
| - 6.60 | -768725  |
| - 5.58 | -712169  |
| - 4.57 | - 641124 |
| - 3.55 | - 549469 |
| - 2.54 | - 430091 |
| - 1.52 | - 277990 |
| - 0.50 | - 96711  |
| 0      | 0        |
| 0.50   | 96711    |
| 1.52   | 277990   |
| 2.54   | 430091   |
| 3.55   | 549469   |
| 4.57   | 641124   |
| 5.58   | 712169   |
| 6.60   | 768725   |
| 7.62   | 815263   |
| 8.63   | 854852   |

### 3.6.1 Typical Outputs

In this thesis the investigation is based on displacement only. So only a displacement output is given. However, other outputs of interest like moment, shear force and reaction can easily be obtained from ANSYS in a similar manner. Fig 3.10 and Fig 3.11 show deflected shapes of a 7 story building frame when the analysis is carried on with and without infill. Similarly Fig 3.12 and Fig 3.13 show deflected shapes of a 11 story building frame when the analysis is carried on with or without infill.

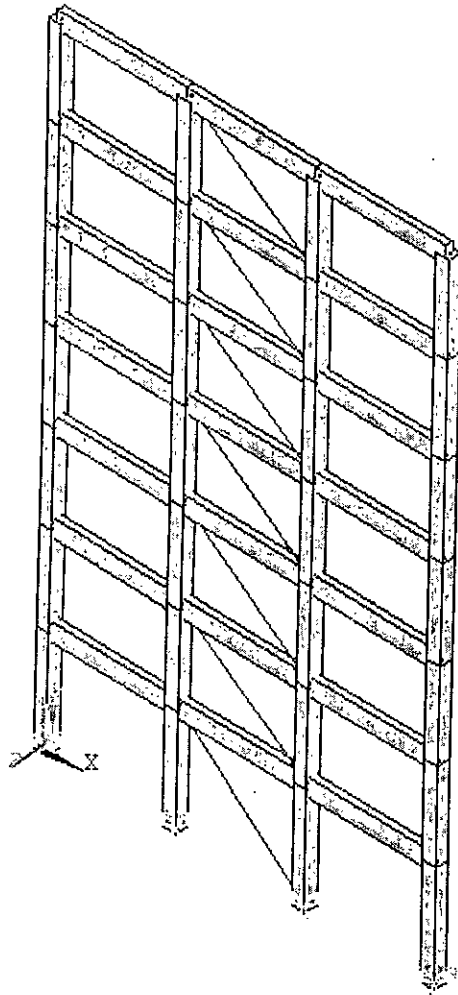


Fig 3.6 Finite element modeling of 7 story infilled frame .

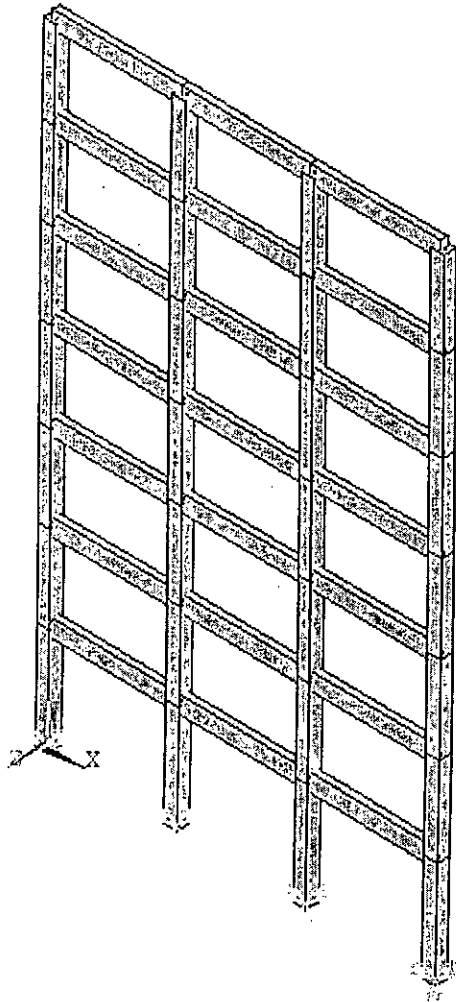


Fig 3.7 Finite element modeling of 7 story frame without infill

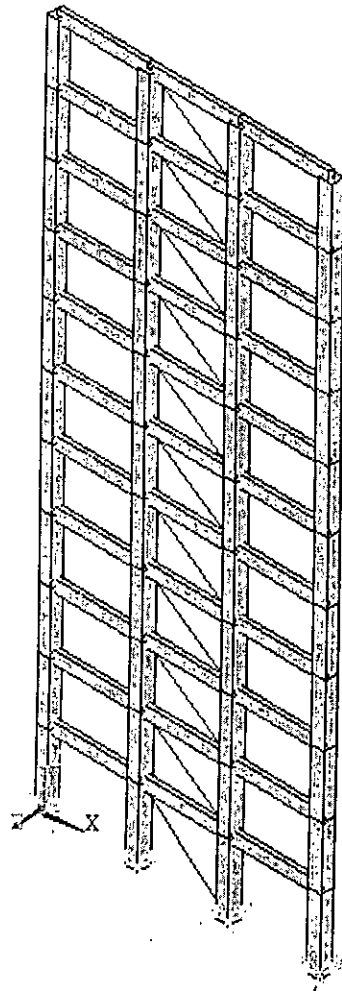


Fig 3.8 Finite element modeling of 11 story infilled frame

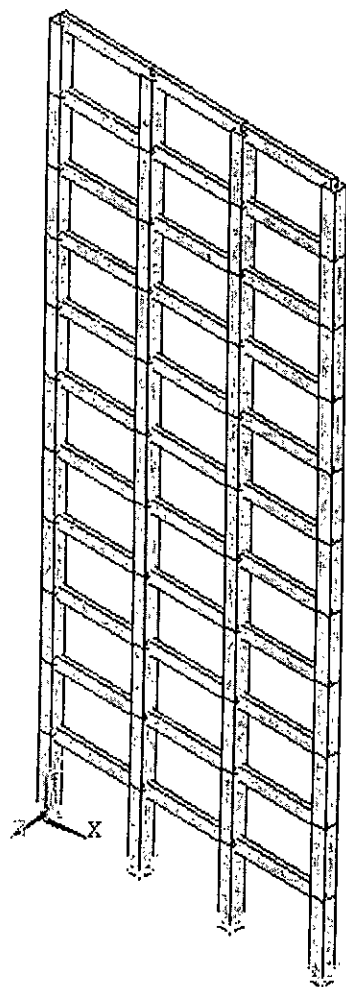


Fig 3.9 Finite element modeling of 11 story frame without infill

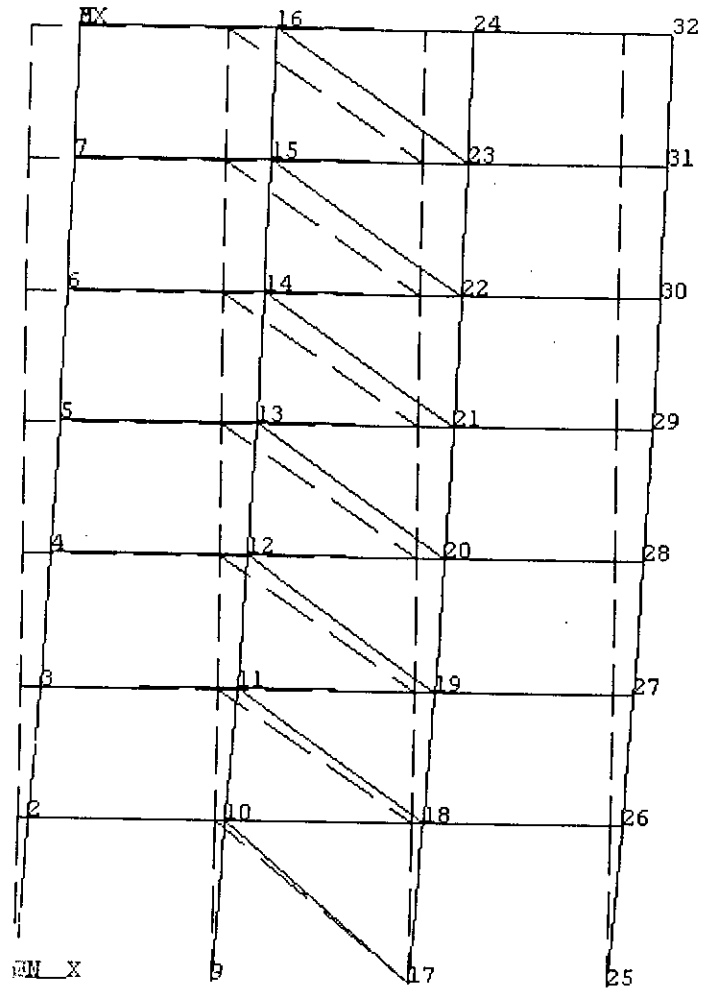


Fig 3.10 Deflected shape of seven story infilled frame

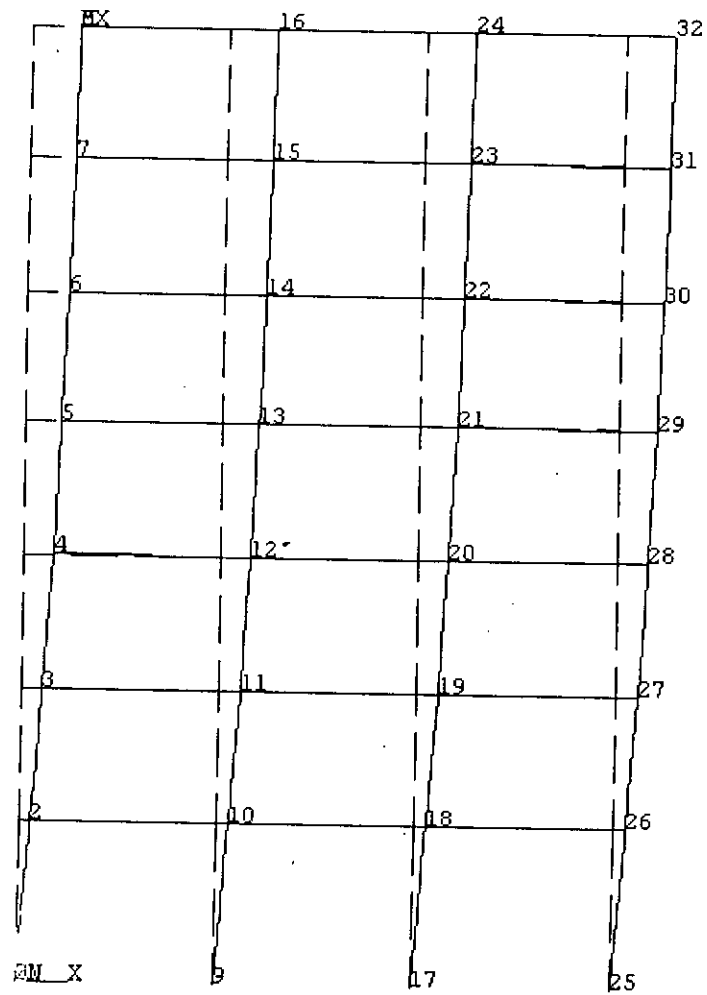


Fig 3.11 Deflected shape of 7 story frame without infill

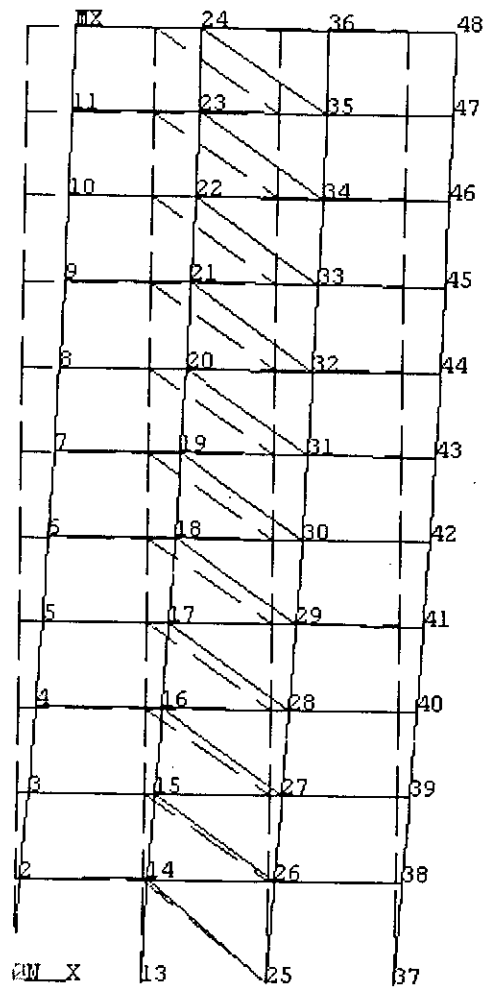


Fig 3.12 Deflected shape of 11 story infilled frame .

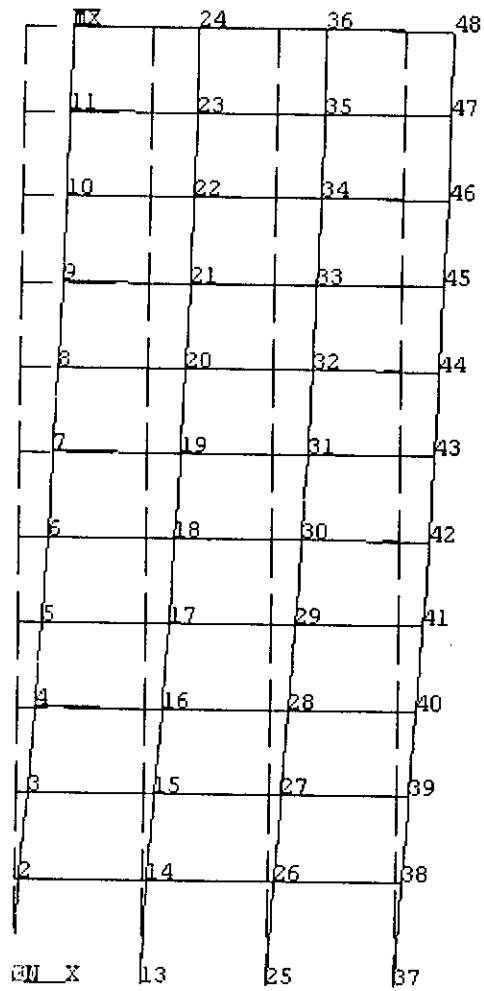


Fig 3.13 Deflected shape of 11 story frame without infill

**Output of 7 story frame**

| Node no | Lateral deflection without infill, mm | Lateral deflection 150 mm infill, mm | Lateral deflection 250 mm infill, mm |
|---------|---------------------------------------|--------------------------------------|--------------------------------------|
| 1       | 0                                     | 0                                    | 0                                    |
| 2       | 5.29                                  | 2.55                                 | 2.08                                 |
| 3       | 9.84                                  | 4.81                                 | 4.01                                 |
| 4       | 13.81                                 | 6.84                                 | 5.78                                 |
| 5       | 17.10                                 | 8.59                                 | 7.32                                 |
| 6       | 19.61                                 | 9.97                                 | 8.58                                 |
| 7       | 21.26                                 | 10.96                                | 9.51                                 |
| 8       | 22.05                                 | 11.48                                | 10.04                                |

**Output of 11 story frame**

| Node no | Lateral deflection without infill, mm | Lateral deflection 150 mm infill, mm | Lateral deflection 250 mm infill, mm |
|---------|---------------------------------------|--------------------------------------|--------------------------------------|
| 1       | 0                                     | 0                                    | 0                                    |
| 2       | 4.89                                  | 3.09                                 | 2.53                                 |
| 3       | 10.82                                 | 6.73                                 | 5.55                                 |
| 4       | 16.75                                 | 10.34                                | 8.57                                 |
| 5       | 22.34                                 | 13.75                                | 11.49                                |
| 6       | 27.44                                 | 16.90                                | 14.23                                |
| 7       | 31.97                                 | 19.34                                | 16.75                                |
| 8       | 35.87                                 | 22.24                                | 19.00                                |
| 9       | 39.07                                 | 24.36                                | 20.95                                |
| 10      | 41.55                                 | 26.08                                | 22.58                                |
| 11      | 43.28                                 | 27.38                                | 23.87                                |
| 12      | 44.34                                 | 28.21                                | 24.74                                |

## CHAPTER 4

## SENSITIVITY ANALYSIS AND DISCUSSION.

## 4.1 INTRODUCTION

The essential theory of infill frame and FE modeling of the infill frame has been described briefly in chapter 2 and chapter 3 respectively. In this chapter an investigation is performed based on those two chapter for various parametric condition. This chapter aims at the studying the sway behavior of frame, when the frame is modeled with or without infill at constant lateral loading. The strut stiffness influence the displacement behavior of infilled frames.

## 4.2 SYUDY PARAMETERS

There are a few material and geometric parameters which influence the behavior of infilled frames. These parameters are as follows:

Co-efficient of friction,  $\mu$

Masonry compressive strength,  $f'_m$

Panel aspect ratio, ( $h/l$ )

Column stiffness,

Wall thickness,  $t$  and

Masonry ultimate strain,  $\epsilon'_m$

The general idea of parametric study for a number of independent parameters embodies the fact that a single instance only one variable should be allowed to vary while other parameters are fixed at some standard value within its range. If we allow two or more parameters to vary at the same time it would cause a confusion in the results of the sensitivity analysis. Hence our investigation specifies a fixed range for all the variables within which the actual work of sensitivity analysis is carried out.

#### 4.2.1 Friction Co-efficient, $\mu$

The friction between masonry and beam or column face is considered. Typical value of this friction co-efficient is 0.65, where it is studied for different values in the range of 0.5 to 1.10.(Hossain.M.1997).

#### 4.2.2 Masonry Compressive Strength, $f'_m$

Masonry compressive strength is a direct indication of the effect of infill on the sway characteristics of the frame. In this study a typical value of masonry compressive strength is 12 Mpa and it is studied for the different values in the range 8 to 16 Mpa.(Hossain.M. 1997).

#### 4.2.3 Panel Aspect Ratio ( $h/l$ )

Panel aspect ratio is the direct indication of the effect of frame sway characteristics when the frame is modeled with or without infill. In infilled frames the infill stiffness greatly depends on panel aspect ratio. So it is an important parameter for infilled frames analysis. The panel aspect ratio depends on floor height  $h$  and span length  $l$  of the frame. In this analysis the floor height  $h$  is 3650 mm for ground floor and 3000 mm for other floors. The span length  $l$  has a typical value of 4500 mm and it is studied for different values in the range between 3000 mm to 6000 mm.

#### 4.2.4 Column Stiffness

Column stiffness mainly indicate the area moment of inertia of column. To find a dimensionless value of column stiffness, we divide the inertia of column in the loading direction by the area moment of inertia of infill. In this analysis a typical value of column size is 600mm×600mm for 11 story frame and for 7 story frame the column size is 450mm×450mm. In this analysis behavior of infilled frames studied by varying the column size in the loading direction. For 7 story this variation ranges from 350mm to 550mm and for 11 story from 500mm to 700mm increasing at the rate of 50mm.

#### 4.2.5 Wall Thickness, $t$

Wall thickness also a direct indication of the infill stiffness. The compressive strength of masonry has great influence on the sway characteristics of the masonry infilled frames, described in Art. 4.2.2. Generally 5 inch and 10 inch thick walls are used in the building structures. So we studied two wall thickness 150 mm and 250 mm in this analysis, which are very close to 5 inch and 10 inch general wall thickness.

#### 4.2.6. Masonry Ultimate Strain

Masonry ultimate strain is a proportional value of displacement or sway of the infilled frames against lateral loading. In this analysis a typical value of masonry ultimate strain is 0.002 and it is studied for the different values in the range from 0.0016 to 0.0026. (Hossain.M, 1997)

### 4.3 OBSERVATION PARAMETERS

The parameters described in article 4.2 have great influence on the different characteristics and parameters of infill. In this analysis the study carried on the deflection or sway characteristics of the infilled frames and the stiffness  $K_\theta$  of the equivalent strut. These two characteristics are chosen as the observing parameters. The effect of various study parameters on this two quantities are studied, each presented in the next article.

### 4.4 RESULTS AND DISCUSSION

In this section the detail results of the sensitivity analysis are presented. Basically two parameters were observed for the variation of different study parameters as mentioned in article 4.3.

#### 4.4.1. Sensitivity of $K_\theta$

Initial stiffness of the diagonal strut is the single most important parameter for the infill. Therefore its variation was studied for different values of masonry ultimate strain  $\epsilon'_m$ , masonry compressive strength  $f'_m$  and co-efficient of friction between

infill and frame interface  $\mu$ . Following these, fig 4.1 through 4.5 represents the sensitivity of  $K_\theta$  with respect to these parameters.

#### **Effect of masonry ultimate strain $\varepsilon'_m$ on diagonal strut stiffness $K_\theta$**

Fig 4.1 shows the sensitivity of diagonal strut stiffness  $K_\theta$  with respect to the variation of ultimate masonry strain  $\varepsilon'_m$ . From this figure it can be understood that stiffness of the strut decreases with increasing the magnitude of the ultimate masonry strain.

#### **Effect of compressive strength of masonry $f'_m$ on diagonal strut stiffness $K_\theta$**

Fig 4.2(a) and 4.2(b) shows the sensitivity of diagonal strut stiffness  $K_\theta$  for different values of masonry compressive strength  $f'_m$  for wall thickness of 250 mm and 150mm respectively. It is observed that diagonal strut stiffness  $K_\theta$  increasing with the increasing compressive strength of masonry  $f'_m$ . For 250 mm infill thickness the rate of increase is higher upto 16 MPa, than it becomes constant.

#### **Effect of co-efficient of friction $\mu$ on diagonal strut stiffness $K_\theta$**

Fig 4.3(a) and 4.3(b) shows the sensitivity of diagonal strut stiffness  $K_\theta$  with respect to the to the variation of co-efficient of friction between frame and infill interface  $\mu$  for wall thickness 150 mm and 250 mm respectively. From fig 4.3 (a) it is observed that the co-efficient of friction  $\mu$  has no significant effect on strut stiffness  $K_\theta$  for a particular value of masonry strain. From fig 4.3 (b) it is observed that the diagonal strut stiffness  $K_\theta$  increasing with the co-efficient of friction  $\mu$  up to a certain limit after which  $K_\theta$  becomes constant. It may be concluded that the co-efficient of friction  $\mu$  has no significant effect on strut stiffness  $K_\theta$ .

#### **Effect of relative column stiffness on diagonal strut stiffness $K_\theta$**

Fig 4.4(a) and 4.4(b) shows the sensitivity of diagonal strut stiffness  $K_\theta$  with the relative column stiffness for wall thickness 150mm and 250mm respectively. From fig 4.4(a) it can be understood that the relative column stiffness has no significant effect on diagonal strut stiffness. But it is clear that the diagonal strut stiffness  $K_\theta$  for

11 storied frame is higher than the 7 with frame. Fig 4.4(b) indicates that  $K_\theta$  increases at a slow rate for both 11 story and 7 story building when the infill thickness is 250 mm.  $K_\theta$  does not significantly depend on column stiffness.

#### **Effect of panel aspect ratio on diagonal strut stiffness $K_\theta$**

Fig. 4.5 (a) and fig 4.5(b) show the effect of panel aspect ratio on diagonal strut stiffness for 7 and 11 story building frames respectively. Diagonal strut stiffness decreases gradually with the increase of panel aspect ratio both for 7 and 11 story frames when infill thickness is 250 mm. Diagonal strut stiffness decreases gradually with the increase of panel aspect ratio more than 0.60 but decreases suddenly at a high rate with the decrease of panel aspect ratio less than 0.60 both for 7 and 11 story when infill thickness is 150 mm. So, it is clear that 150 mm infilled frame is inactive as a diagonal strut for panel aspect ratio less than 0.60.

#### **4.4.2 Sensitivity Study of Deflection**

The main purpose of this analysis is to determine the lateral deflection under lateral load when the analysis is carried on with or without infill for various parametric condition. Therefore the variation of deflection was studied for different values of co-efficient of friction between frame and infill interface  $\mu$  masonry compressive strength  $f'_m$  panel aspect ratio, relative column stiffness and masonry ultimate strain  $\epsilon'_m$ . The following figure from 4.6 through 4.10 represents the sensitivity of lateral deflection with respect to these parameters.

#### **Effect of co-efficient of friction $\mu$ on deflection**

From fig 4.6(a) and 4.6(b) it is observed that the variation of co-efficient of friction between frame and infill interface  $\mu$  has no significant effect on deflection both for 11 story and 7 story infilled frame respectively. It can be observed that the deflection decreases with the increase of wall thickness.

#### **Effect of masonry compressive strength $f'_m$ on deflection**

From fig 4.7(a) and 4.7(b) it is understood that, when the wall thickness increases the lateral deflection slightly decrease both for 11 story and 7 story infilled

frame respectively. It can be also understood that the effect of  $f'_m$  is insignificant on lateral deflection.

#### **Effect of panel aspect ratio on deflection.**

Fig 4.8(a) and 4.8(b) shows the variation of deflection with panel aspect ratio for 7 storied and 11 storied frame respectively. From these figures it is clearly observed that, if panel aspect ratio increase the deflection increases in the presence of infill both in 7 storied and 11 storied frame for the value of panel aspect ratio more than 0.60. For the value of panel aspect ratio less than 0.60 deflection increases suddenly at a very high rate for 150mm infill and gently for 250mm infill. But for frames without infill the deflection decreases throughout with increase of panel aspect ratio. It is clear that 150 mm infilled panel can not reduce deflection when panel aspect ratio is less than 0.60.

#### **Effect of relative column stiffness on deflection**

Fig 4.9(a) and 4.9(b) shows the variation of lateral deflection with the relative column stiffness for 150mm and 250mm wall thickness respectively. These figures indicate that the lateral deflection decreases with the increase of column stiffness. The overall effect is not very significant both for 11 story and 7 story frame. But it is clear that the deflection is much more higher when the wall thickness decreases.

#### **Effect of masonry ultimate strain $\epsilon'_m$ on deflection.**

The effect of masonry ultimate strain  $\epsilon'_m$  on lateral deflection shown in fig 4.10(a) and 4.10(b) for 11 storied and 7 storied frame respectively. From these figures it is clearly understood that, if masonry ultimate strain  $\epsilon'_m$  increase the deflection also increases both for 150mm and 250mm wall thickness.

### **4.5 BEHAVIOUR OF FRAME IN PRESENCE OF INFILL**

Fig 4.11 (a) and 4.11(b) shows the normalized deflected profile of the two building under study. Only the deflection in the left side nodes is plotted. It is

observed that there is a very significant difference in deflection between frames with infill and without infill. Infill frame produce deflection which is as much as 55 percent smaller than the deflection without infill. In all cases the deflection of infill frame was at least 40 percent smaller than the frame without infill. This clearly indicates that in the conventional method of calculating the lateral deflection of RC frames the deflection is significantly overestimated.

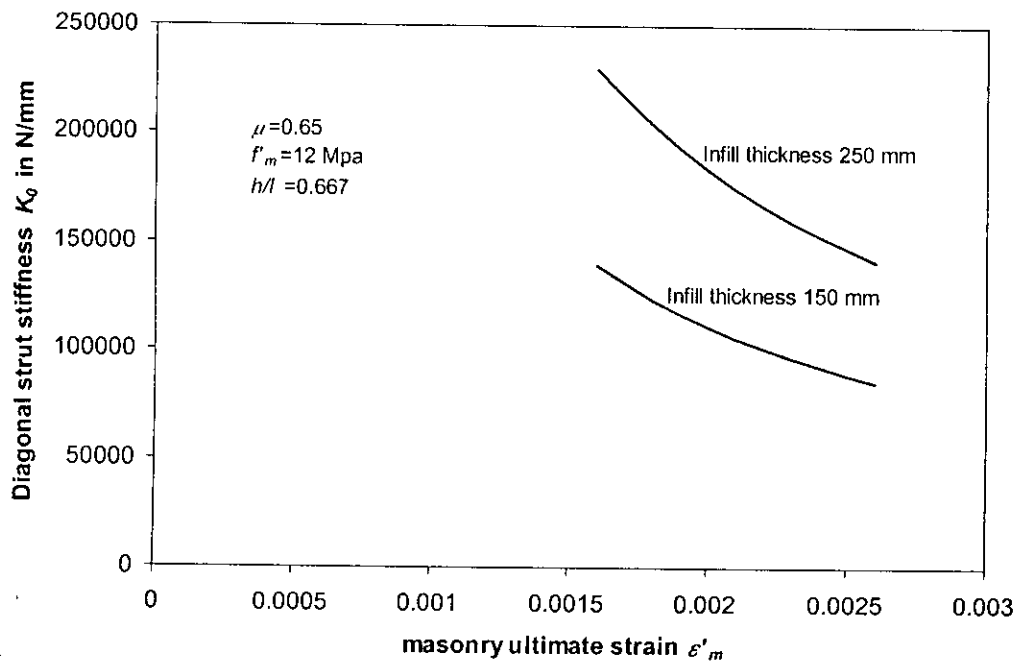


Fig. 4.1 Variation of diagonal strut stiffness with masonry ultimate strain  $\epsilon'_m$  for 11 storied frame.

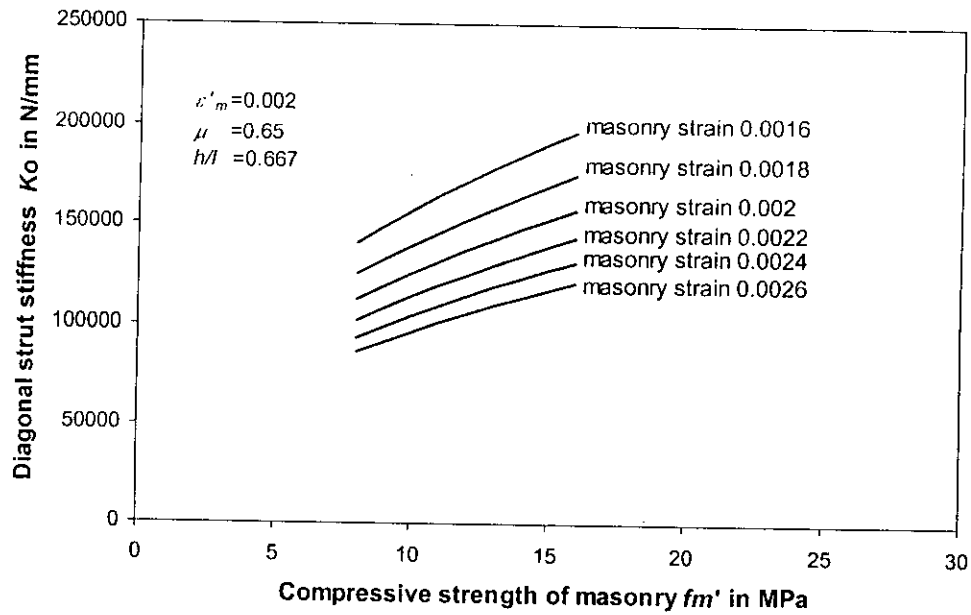


Fig 4.2 (a) Variation of diagonal strut stiffness with compressive strength of masonry when infill thickness is 250 mm.

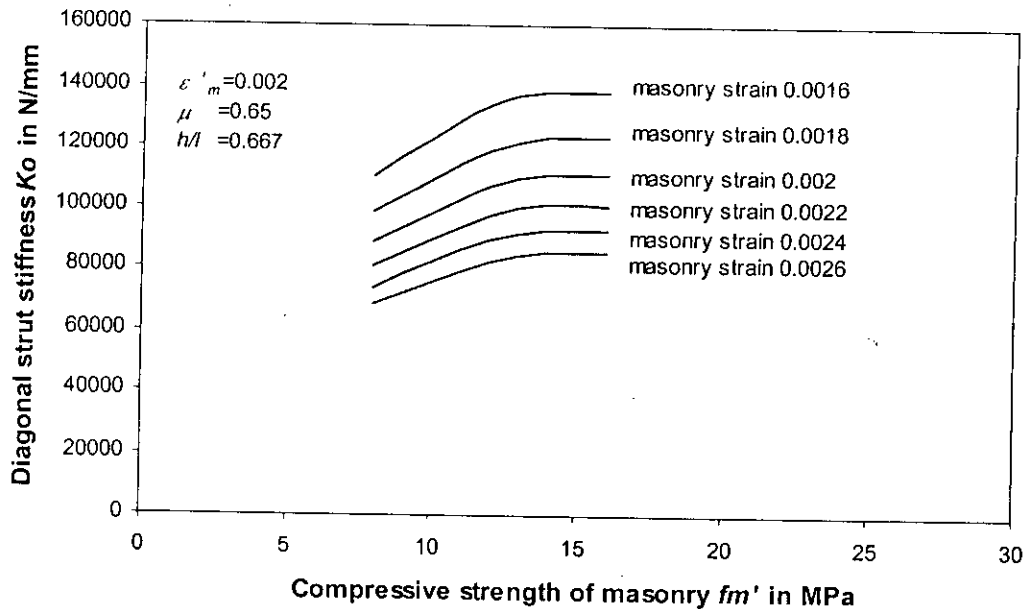


Fig 4.2 (b) Variation of diagonal strut stiffness with compressive strength of masonry when infill thickness is 150 mm.

TS 796

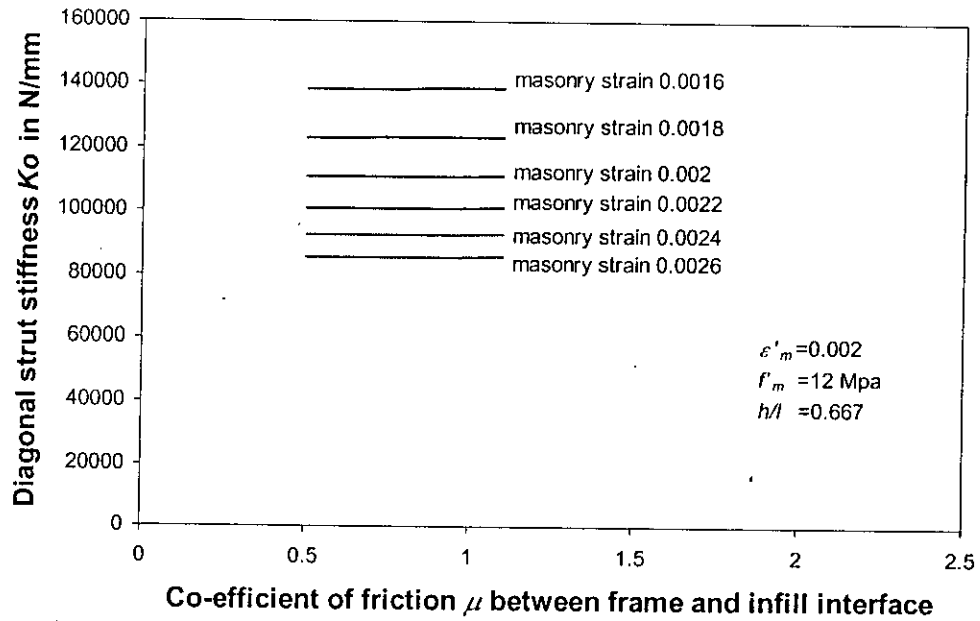


Fig 4.3 (a) Variation of diagonal strut stiffness  $K_0$  with co-efficient of friction between frame and infill interface for 150 mm infilled frame.

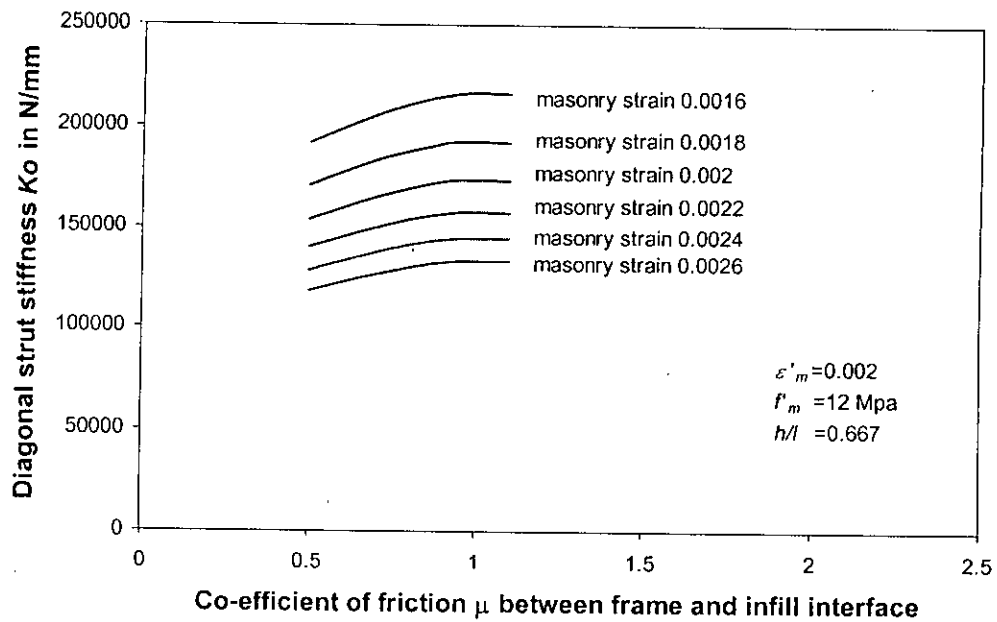


Fig 4.3 (b) Variation of diagonal strut stiffness  $K_0$  with co-efficient of friction between frame and infill interface for 250 mm infilled frame.

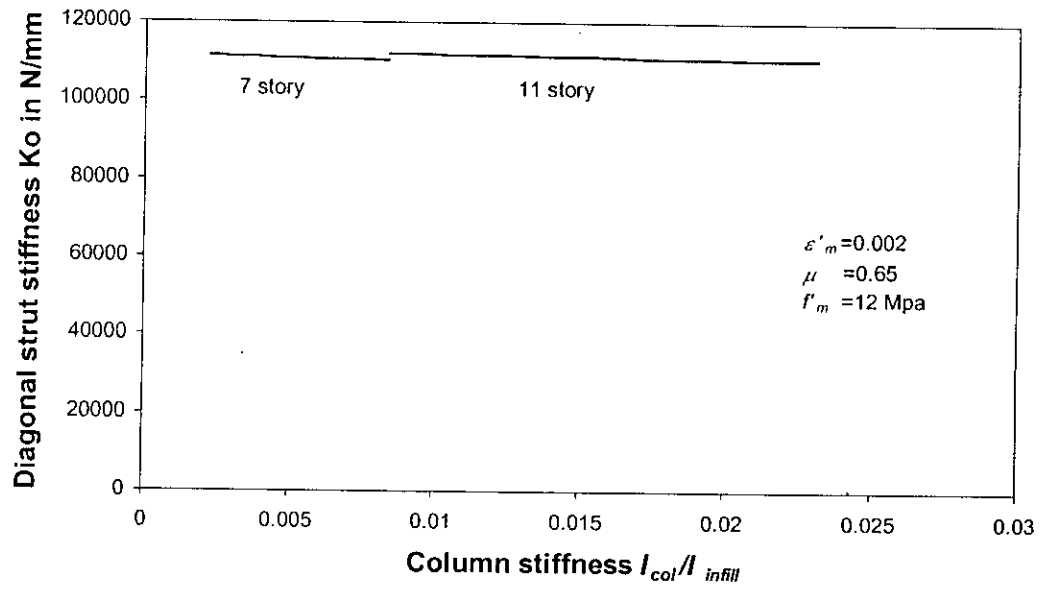


Fig. 4.4(a) Variation of diagonal strut stiffness  $K_0$  with column stiffness for 150 mm infilled frame.

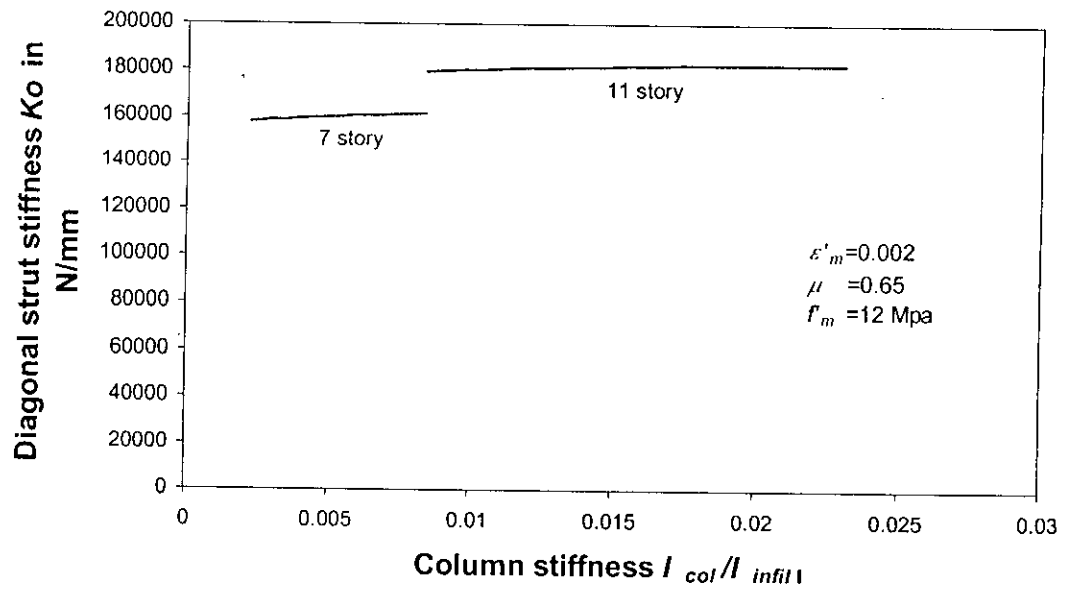


Fig. 4.4(b) Variation of diagonal strut stiffness  $K_0$  with column stiffness for 250 mm infilled frame.

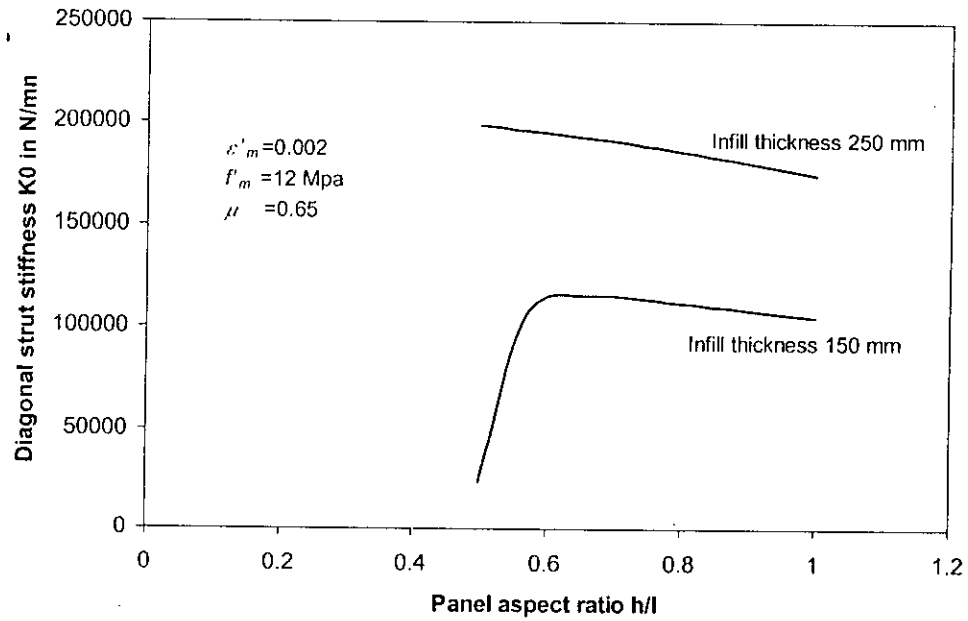


Fig 4.5 (a) Variation of diagonal strut stiffness with panel aspect ratio for 7 storied frame.

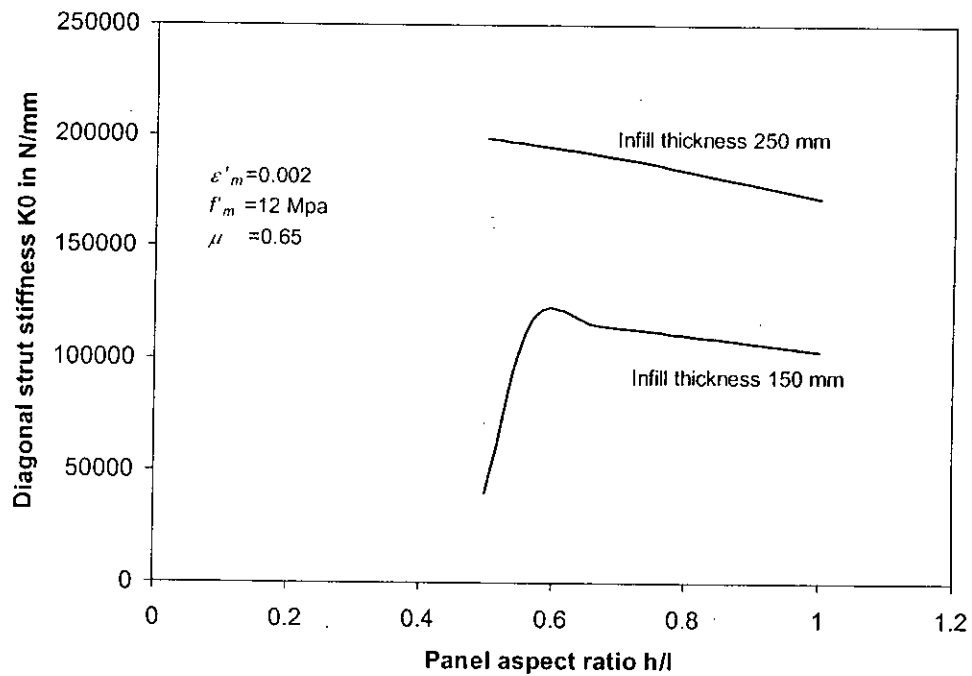


Fig 4.5 (b) Variation of diagonal strut stiffness  $K_0$  with panel aspect ratio for 11 storied frame.

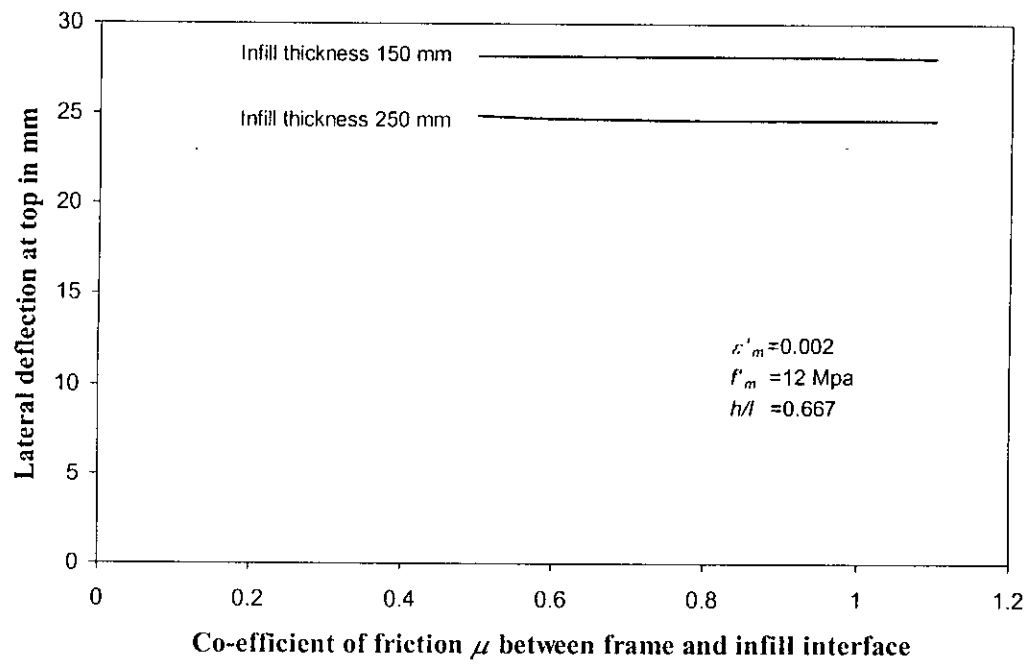


Fig 4.6(a) Variation of deflection with co-efficient of friction  $\mu$  for 11-story frame.

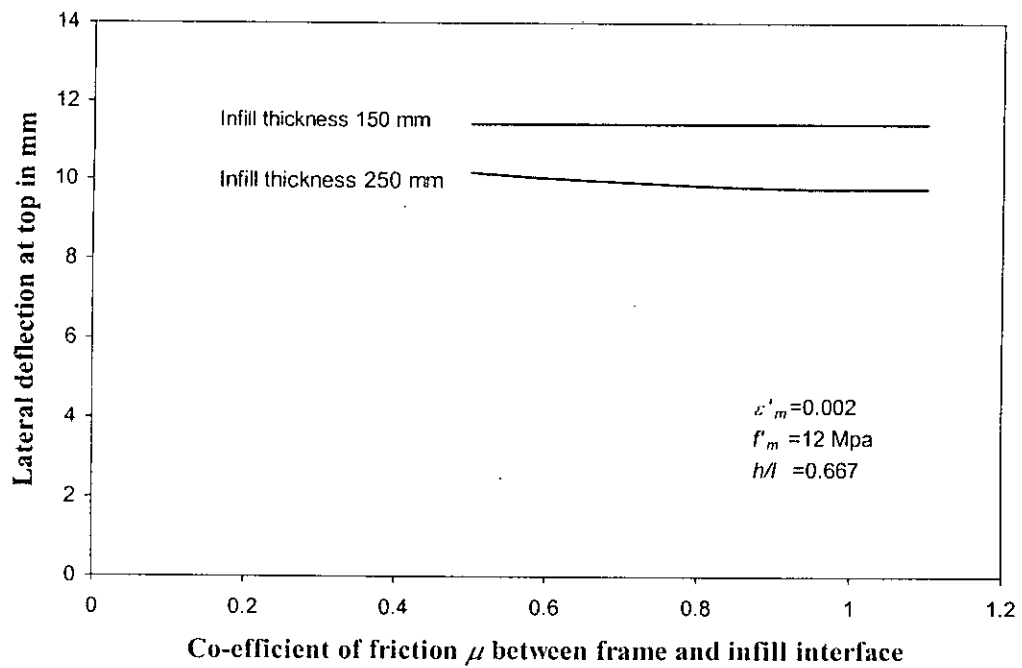


Fig. 4.6(b) Variation of deflection with co-efficient of friction  $\mu$  for 7-story frame.

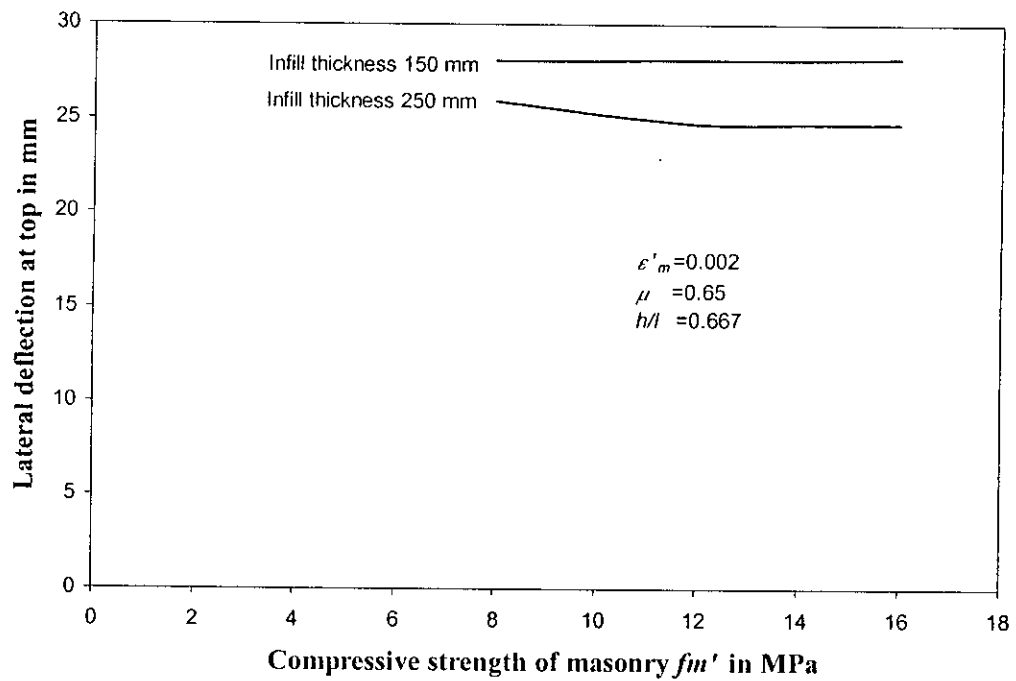


Fig. 4.7(a) Variation of deflection with compressive strength of masonry  $f_m'$  for 11 storied frame.

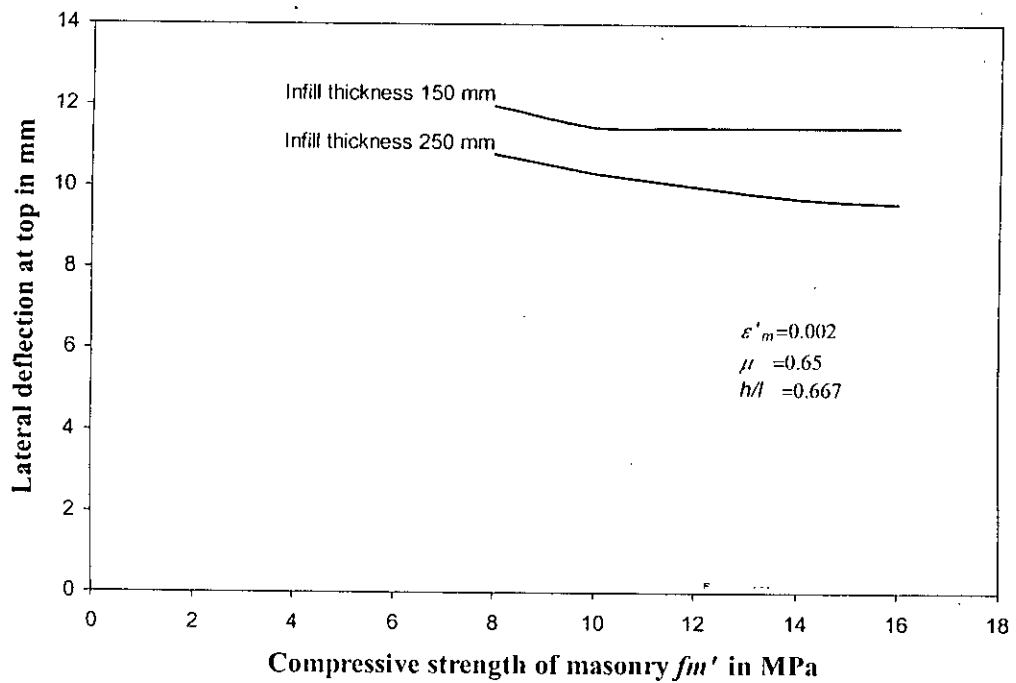


Fig. 4.7(b) Variation of deflection with compressive strength of masonry  $f_m'$  for 7 storied frame.

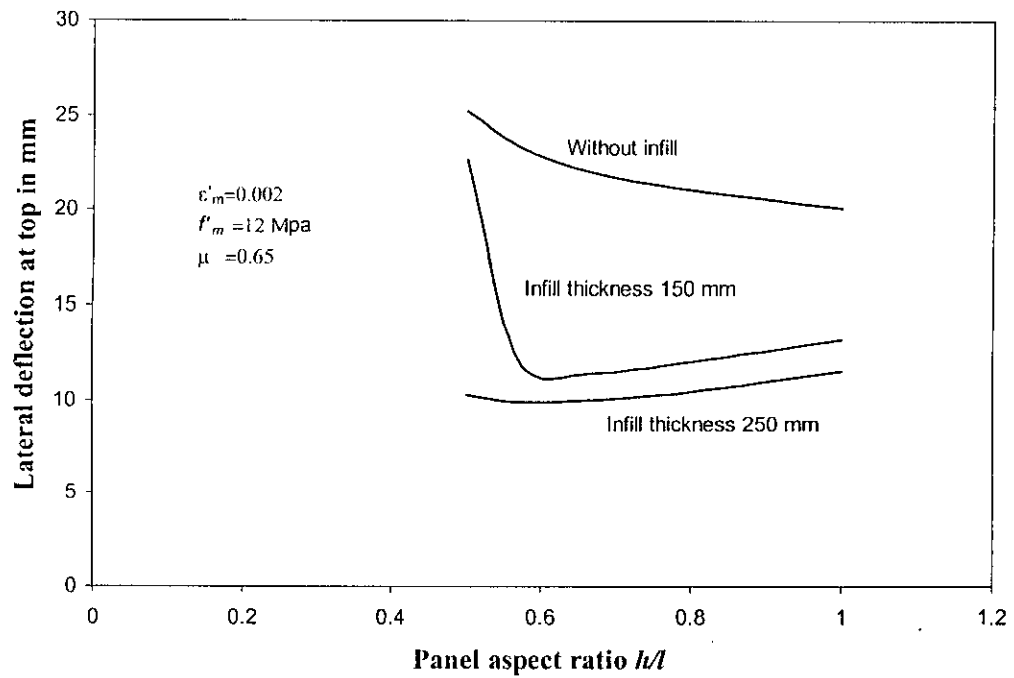


Fig. 4.8(a) Variation of deflection with panel aspect ratio for 7 storied frame.

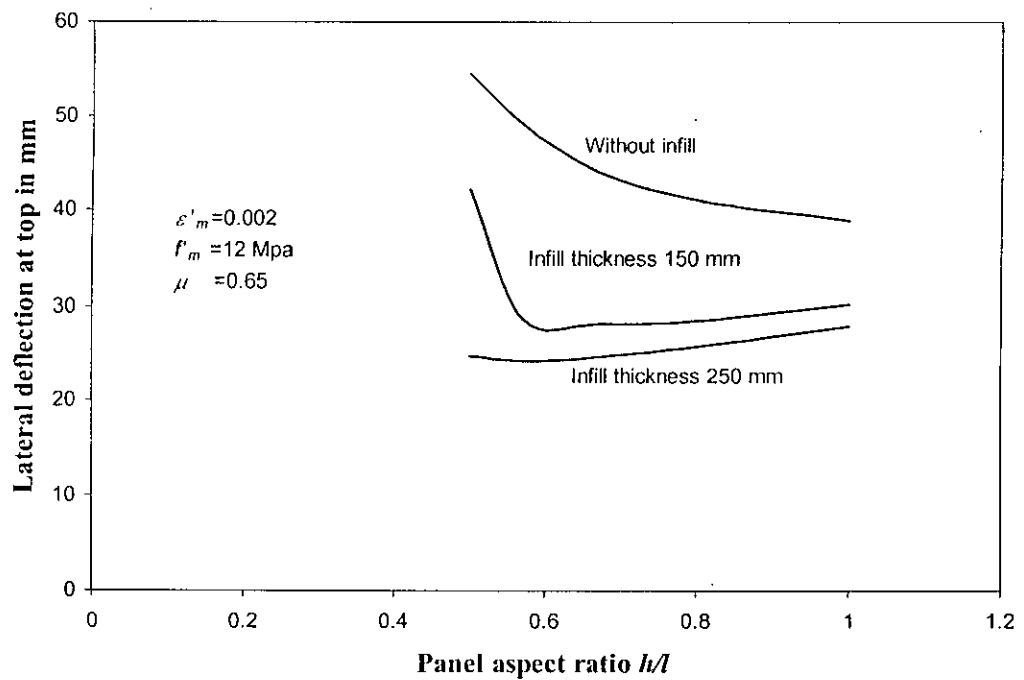


Fig. 4.8(b) Variation of deflection with panel aspect ratio for 11 storied frame.

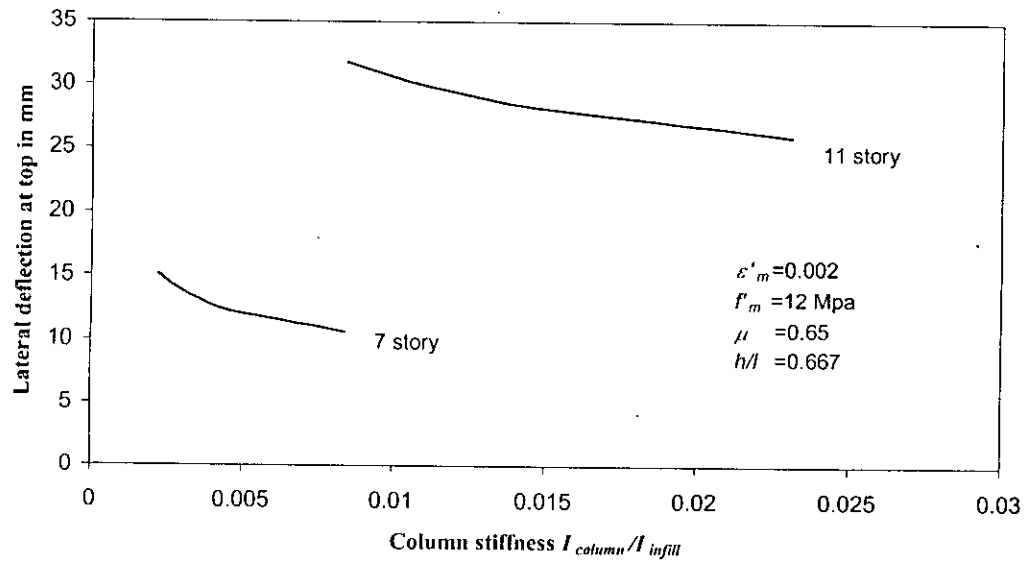


Fig. 4.9(a) Variation of deflection with column stiffness for infill thickness 150 mm.

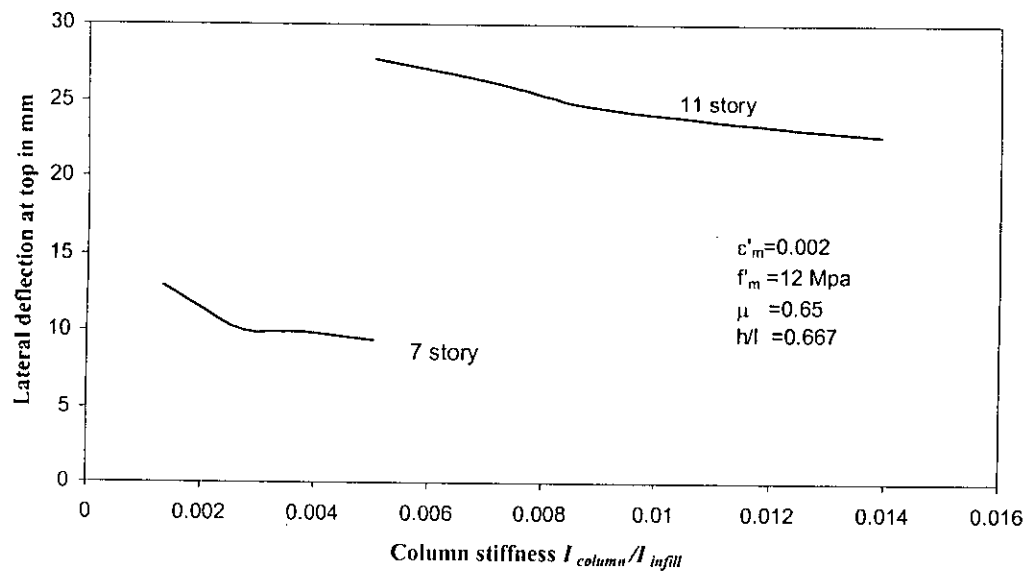


Fig. 4.9(b) Variation of deflection with column stiffness for infill thickness 250 mm.

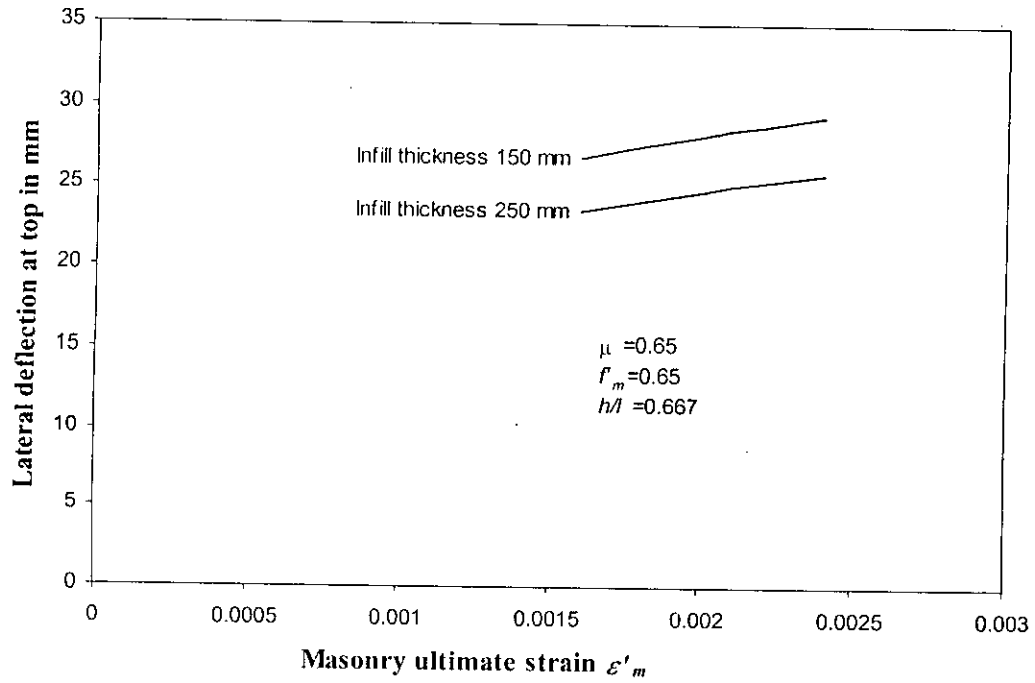


Fig. 4.10(a) Variation of deflection with masonry ultimate strain  $\epsilon'_m$  for 11 storied frame.

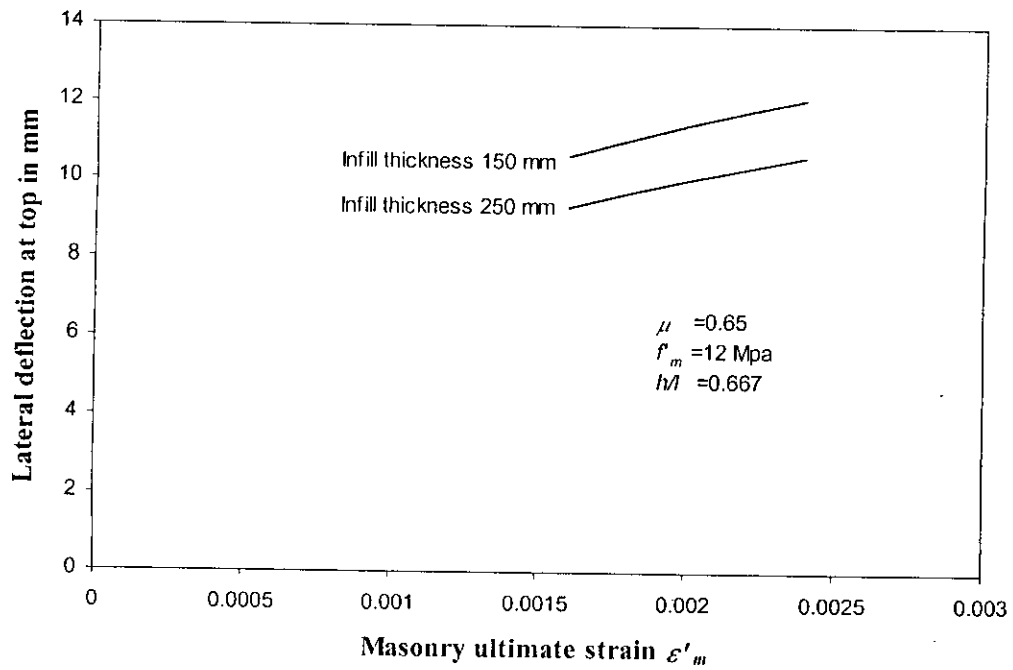


Fig. 4.10(b) Variation of deflection with masonry ultimate strain  $\epsilon'_m$  for 7 storied frame.

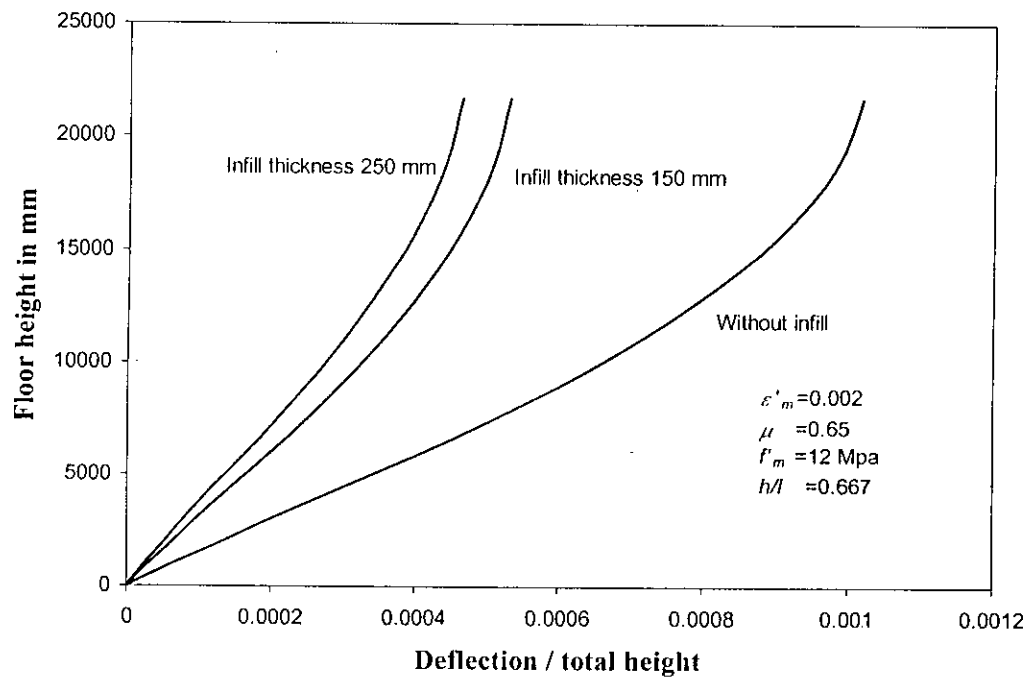


Fig. 4.11(a) Variation of floor height with deflection/total height for 7 storied frame.

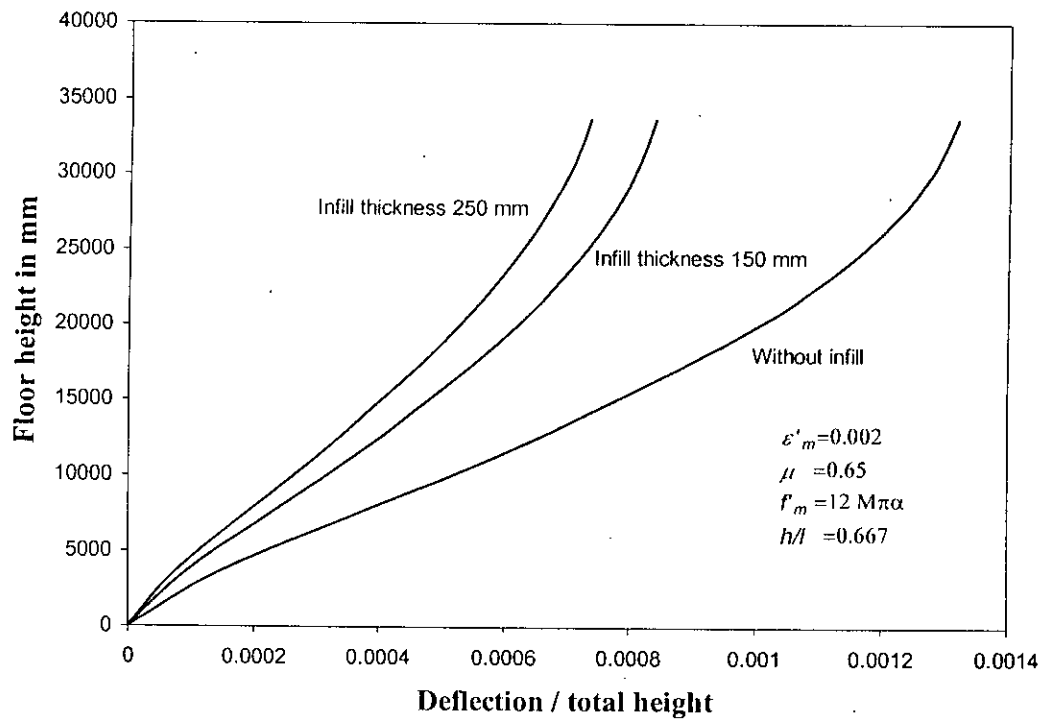


Fig. 4.11(b) Variation of floor height with deflection/total height for 11 storied frame.

---

**CHAPTER 5**  
**CONCLUSIONS**

---

**5.1 GENERAL**

In the context of Bangladesh moderately tall building story ranges from 7 through 15. The Bangladesh National Building Code (BNBC 1993) provides wind load specification which is applicable to single story buildings also. Recent history of cyclonic storms as well as earthquake incidences suggest that any multistoried building should be analysed and designed for lateral loads. It is well recognized that the wind load specifications of Bangladesh National Building Code is one of the most stringent and highly conservative wind load specification in the world. As a result the lateral sway produced by wind load analysis as per BNBC specification usually turns out to be very high for frame structures of ordinary configuration. In order to keep the lateral deflection within acceptable limits (e.g. 1/480 th of the building height) the columns and beams have to be built with larger sections rendering the structure uneconomical. This situation can be improved if the structural effect of brick masonry infills, which are frequently used in RC framed structures in Bangladesh, is considered. In this study it has been shown that the lateral deflections of RC frames are dramatically reduced if the structural effect of the infill is considered in the analysis. In the present investigation the infills are modeled as diagonal struts following the theory of Seneinejad and Hobbs (1995). In order to simulate a realistic behavior of the strut a non-linear force vs. displacement relation has been suggested (equation 2.17) and used. A seven story and an eleven story frame are analysed and their lateral sway characteristics are studied in presence of infill. Then the results have been compared with the same obtained from frames without infill. It has been observed that lateral sway is significantly reduced when infills are considered in the analysis.

**5.2 CONCLUSIONS**

- The findings from the parametric study both for 7 story and 11 story buildings for infill and frame are summarized below:
  - With the increase of masonry ultimate strain  $\varepsilon'_m$ , the diagonal strut stiffness  $K_\theta$  decreases and as such the sway of the structure increases.

- The equivalent strut stiffness  $K_{\theta}$  increases with increasing masonry compressive strength  $f'_m$ . This eventually reduces the lateral sway of the building.
  - Lateral sway decreases with increasing relative column stiffness. However, relative column stiffness has no significant effect on diagonal strut stiffness  $K_{\theta}$ .
  - The co-efficient of friction  $\mu$  between frame and infill has no significant effect on deflection and as well as on diagonal strut stiffness  $K_{\theta}$ .
  - Generally sway of the frame increases with the increase of panel aspect ratio although the magnitude of deflection remains significantly smaller than that without infill. However, when panel aspect ratio is approximately 0.60 or smaller, 150 mm thick infill does not offer significant lateral resistance. In such conditions, the sway is high and tends to be equal with that without infill.
- Sway of frame estimated considering the presence of infill is significantly smaller than that estimated without the presence of infill. The amount of sway reduction depends on the number of infilled panels in the frame. In the present study 33% of the panels contained infills. It has been found that infills can effectively reduce the lateral sway of reinforced concrete structures by as much as 50%.
- In a real life analysis and design of a framed structure, it is difficult to incorporate the infills in the computational model. Therefore after obtaining lateral sway value from a conventional analysis it may be reduced by some amount to get an estimate of the realistic sway value of RC framed structures.

### 5.3 RECOMMENDATION FOR FUTURE INVESTIGATION

In this study a few parameters of infilled frame structure and their influence on lateral sway is studied. However, the study can not be said to be comprehensive due to the limited scope. Further study and investigation can be carried out in the following areas related to infilled frame structures.

- Material and geometric parameters other than those studied in this thesis may be investigated.

- The effect of infill on building design parameters such as bending moment, shear force and axial force in beams and columns may be studied.
- A cost-benefit analysis may be carried out to find out the relative economy that may be achieved if infills are considered as structural elements.
- In this study only 33 % of the panels contained infills. Study may be carried out for various amount of infills ranging from as low as 10 % to as high as 90 %.
- In this thesis infills were distributed in the frame in a regular pattern. A similar study may be carried out with randomly distributed infills.
- Considering the present trend of keeping ground floor free of infills for parking, a study may be carried out with infills only on upper floors keeping the ground floor free from any infills.

## References :

- ANSYS Elements Reference, 000853, Ninth Edition, SAS IP, inc. 1997.
- Bangladesh National Building Code (BNBC), Housing and Building Research Institute and Bangladesh Standards and Testing Institution, 1993.
- Hossain.M, "Non linear finite element analysis of Wall-Beam structures," Ph.D.thesis, Department of Civil Engineering, BUET,1997.
- J.C.J. Schellekens and R.de Borst, "The use of the Hoffman yield criterion in finite element analysis of anistropic composites," Comput.Struct.,37,1087-1096 (1990).
- J.F. Besseling, "A theory of elastic, plastic and creep deformations of an initially isotropic material showing anistropic strain-hardening, creep recovery and secondary creep," J.Appl.Mech.,22,529-536 (1958).
- Lourenco, P. B., Brost, R. D. and Rots, J. G. "A Plane Stress Softening Plasticity Model For Orthotropic Materials", International Journal For Numerical Methods In Engineering, Vol. 40, 4033-4057 (1997).
- Madan, A. Reinhorn, A. M. ,Fellow ,ASCE, Mander, J. B., Member, ASCE, and Valles, R. E. "Modeling of Masonry Infill Panels For Structural Analysis", American Soc. of Civ. Engrs. (ASCE), Journal of Structural Engineering, Vol. 123, No. 10, October 1997, 1295-1297.
- O.Hoffman, "The brittle strength of orthotropic materials," J.Composit Mat.,1,200-206 (1967).
- Papia, M. "Analysis of Infilled Frames Using a Coupled Finite Element And Boundary Element Solution Scheme", International Journal For Numerical Merhods In Engineering ,Vol. 26, 731-742 (1998).
- R.de Borst and P.H. Pheenstra, "Studies in anistropic plasticity with reference to the Hill criterion," Int.J.Numer.Meth.Engng.,29,315-336 (1990).
- R.Hill, "A theory of the yielding and plastic flow of anistropic metals," Proc.Roy.Soc.,(London) A193,281-288 (1948).
- Saneinejad, A.and Hobbs, B. "Inelastic Design of Infilled Frames",American Soc, of Civ, Engrs. (ASCE), Journal of Structural Engineering. Vol. 121, No. 4. April 1995. 634-643.
- Smith. B. S. and Coull, A. "Infilled-Frame Structures", Tall Building Structures Analysis And Design, John Wiley & Sons, inc. 168-174.
- Winter, G. and Nilson, A. H. (1987), "Design of Concrete Structures", McGraw Hill, 10th Edition.

